SCIENCE INSTITUTE
RH - 11 - 95
University of Iceland
Dunhagi 3, 107 Reykjavík

NORDIC VOLCANOLOGICAL
INSTITUTE 9504
University of Iceland
101 Reykjavík

GPS Experiments in the Eastern Volcanic Zone, South Iceland, in 1994

Sigurjón Jónsson, Páll Einarsson, Freysteinn Sigmundsson,
Karl Pálsson and Halldór Ólafsson

Reykjavík 1995

Contents

Chapter 1

Introduction

The 1994 GPS-campaign in the Eastern Volcanic Zone, South Iceland, was a cooperative work of the Nordic Volcanological Institute and the Science Institute of the University of Iceland. A total of 75 points were measured, divided into three experiments:

1. Monitoring of the Mýrdalsjökull volcanoes (Katla and Goðabunga) and Eyjafjallajökull, 17 points. Most of them have been measured before, but a few new points were added around Eyjafjallajökull because of seismic unrest there in the spring of 1994. The measurements were made from May 27 to June 6, and September 18-22. The Reynisfjall control point was used as a base station.

2. Monitoring of the Hekla volcano, 19 points. Most of these points were also measured in 1993, but tilt measurements indicate that Hekla may be inflating, and it is of considerable interest to capture the crustal deformation field during an inflation period.

3. Measurements of a network across the Eastern Volcanic Rift Zone, 42 points. This network included all GPS-points measured in previous GPS-surveys in 1986, 1989, 1991 and 1992, and also a distance profile of 25 points that has been measured several times with a geodimeter, first in 1967. The Hekla and the Eastern Volcanic Rift Zone measurements were conducted from July 18 to July 29 and from August 30 to September 17. The Ísakot control point was used as a reference station.

The location of these networks is displayed in Figure 1.1.

In this report we present information about the measurements and the data processing for the third experiment. This is followed by the basic processing results; the coordinates of occupied stations in the Eastern Volcanic Rift Zone.

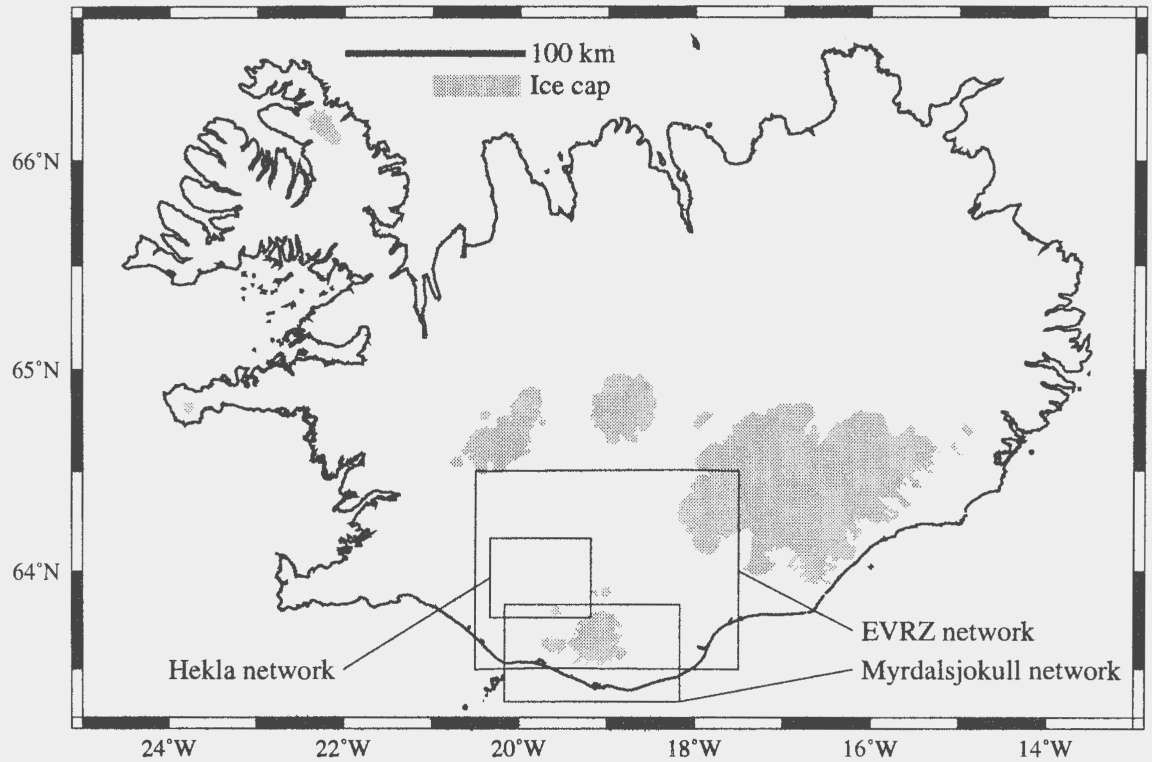

Figure 1.1: Map of Iceland. Squares indicate location of networks of the Hekla Volcano, Mýrdalsjökull and the Eastern Volcanic Rift Zone (EVRZ).

Chapter 2

Measurements

2.1 Equipment and Participants

Three Trimble 4000 SST GPS-receivers, owned by the Nordic Volcanological Institute were used in the measurements. One vehicle was used for most of the work. The Science Institute provided jeep for part of the time and the Nordic Volcanological Institute also provided a vehicle for this work. The National Power company, Landsvirkjun, provided accommodation for most of the work in the Hekla area and in the Eastern Volcanic Rift Zone. Mountain huts and a tent were also used by the measurement group when access to points became more difficult. The field work was done by Sigurjón Jónsson and Páll Einarsson from the Science Institute and by Karl Pálsson, Halldór Ólafsson and Freysteinn Sigmundsson from the Nordic Volcanological Institute.

2.2 General Information

Each day consisted of three measurement sessions, each session 7:55 hours long. Session 0 started at 00:00 UTC and sessions 1 and 2 at 8:00 and 16:00, respectively, i.e. the three sessions of the day 199, e.g., were called 199-0, 199-1 and 199-2. The measurement interval was 15 seconds and the satellite elevation mask angle was 15°. Data from all visible satellites were collected, but their number were from four to nine. No meteorological data were collected.

The station Ísakot (ISAK) was used as a reference station for the experiments of Hekla and the Eastern Volcanic Rift Zone, but the station Reynisfjall (REYN) for the Mýrdalsjökull experiment. One receiver was situated on a reference point during each experiment and the other two receivers were moved between benchmarks on session 1 every day. Therefore, each point was usually occupied for two whole sessions (session 2 and 0) and for part of the third

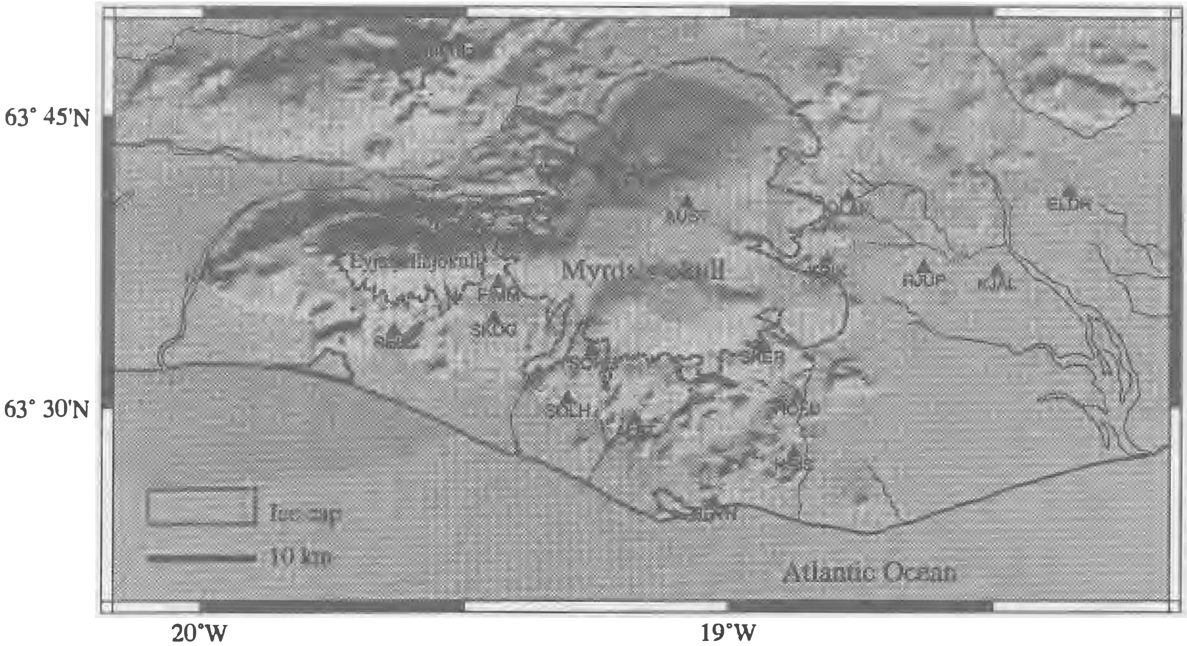

Figure 2.1: The Mýrdalsjökull and Eyjafjallajökull GPS-network, most of the network was measured in 1994.

(session 1), this gave usually 16-22 hours data for each point. The antenna was set up only once at each station.

2.3 The Mýrdalsjökull and Eyjafjallajökull Experiment

The main goal of GPS-measurements around the Mýrdalsjökull volcanoes (Goðabunga and Katla) and Eyjafjallajökull is to monitor these volcanoes. The most recent eruptions in Mýrdalsjökull were in Katla, in 1918 and a possible subglacial eruption in 1955. The volcano has erupted many times during the last centuries, about twice each century. Many earthquakes are observed every year in Mýrdalsjökull and they define two epicentral clusters, in Goðabunga and in Katla (Einarsson, 1991).

The last eruption in the Eyjafjallajökull volcano was in 1821-23. The eruption frequency is significantly lower than in Katla, but the volcano isn't at rest. An unusual earthquake sequence was observed in Eyjafjallajökull in the spring of 1994. Both the Mýrdalsjökull and Eyjafjallajökull volcanoes are ice covered and have the potential to cause great damage. It is therefore of a considerable interest to monitor these volcanoes.

Abbreviation	*Name*	*Inscription*	*Approx. coord.*		
			Lat.	*Lon.*	*H*
REYN	Reynisfjall	OS 7377	63 25 06 N	19 01 38 W	294
ENTA	Enta	Iron rod	63 42 04 N	19 10 56 W	1407
AUST	Austmannsbunga	NE 93 04	63 40 27 N	19 04 50 W	1439
SOHH	Sólheimaheiði	NE 92 14	63 32 54 N	19 15 29 W	787
SOLH	Sólheimar	NE 92 15	63 30 26 N	19 18 19 W	278
KJAL	Kjalnatær	NE 93 06	63 36 58 N	18 29 39 W	132
KRIK	Kötlukriki	726	63 37 35 N	18 48 55 W	367
OLAF	Ólafshaus	746	63 40 48 N	18 46 56 W	290
RJUP	Rjúpnafell	NE 93 03	63 37 08 N	18 37 57 W	186
STEI**	Steinsholt	NE 94 005	63 40 37 N	19 36 30 W	300
HAMR	Hamragarðar	OS 74 87	63 37 20 N	19 59 08 W	160
SELJ**	Seljavellir	NE 94 004	63 33 45 N	19 37 57 W	275
HRIS	Hríshóll	NE 92 02	63 27 38 N	18 52 38 W	240
HOFD	Höfðabrekkuheiði	704	63 30 31 N	18 52 13 W	280
SKOG	Skógaá	OS 74 86	63 34 35 N	19 26 43 W	669
FIMM	Fimmvörðuháls	NE 92 03	63 36 24 N	19 26 15 W	918
ALFT	Álftagróf	NE 92 13	63 29 22 N	19 10 38 W	203
ELDH	Eldhraun	OS 5847	63 41 05 N	18 21 26 W	146
SKER*	Sker	NE 92 01	63 33 11 N	18 56 12 W	750

Table 2.1: GPS control points near Mýrdalsjökull and Eyjafjallajökull. Point marked by * was not measured in 1994. Points marked by ** were established in 1994. H is height above reference ellipsoid, in meters. Abbreviations of inscriptions: OS National Energy Authority, NE Nordic Volcanological Institute.

The original GPS-network around Mýrdalsjökull was mainly established in 1992 and consisted of twelve points. The network was densified and expanded in 1993. Five new points were added, including two points on nunataks within the Mýrdalsjökull ice cap (on Enta (ENTA) and Austmannsbunga (AUST)). The whole network then consisted of 17 points and they were all measured in June 1993, except three, Sker (SKER), Fimmvörðuháls (FIMM) and Skógaá (SKOG), because of closed tracks.

Two new points were added to the network in 1994 and now the network includes 19 points, see Table 2.1 and Figure 2.1. The whole network was measured in 1994, except one point, Sker (SKER). The measurements were made from May 27 to June 6 and September 18-22, see Table A.1. The Reynisfjall (REYN) control point was used as a reference station. The GPS-points measured around Mýrdalsjökull and Eyjafjallajökull in 1992-94 are shown in Figure 2.2, a-c.

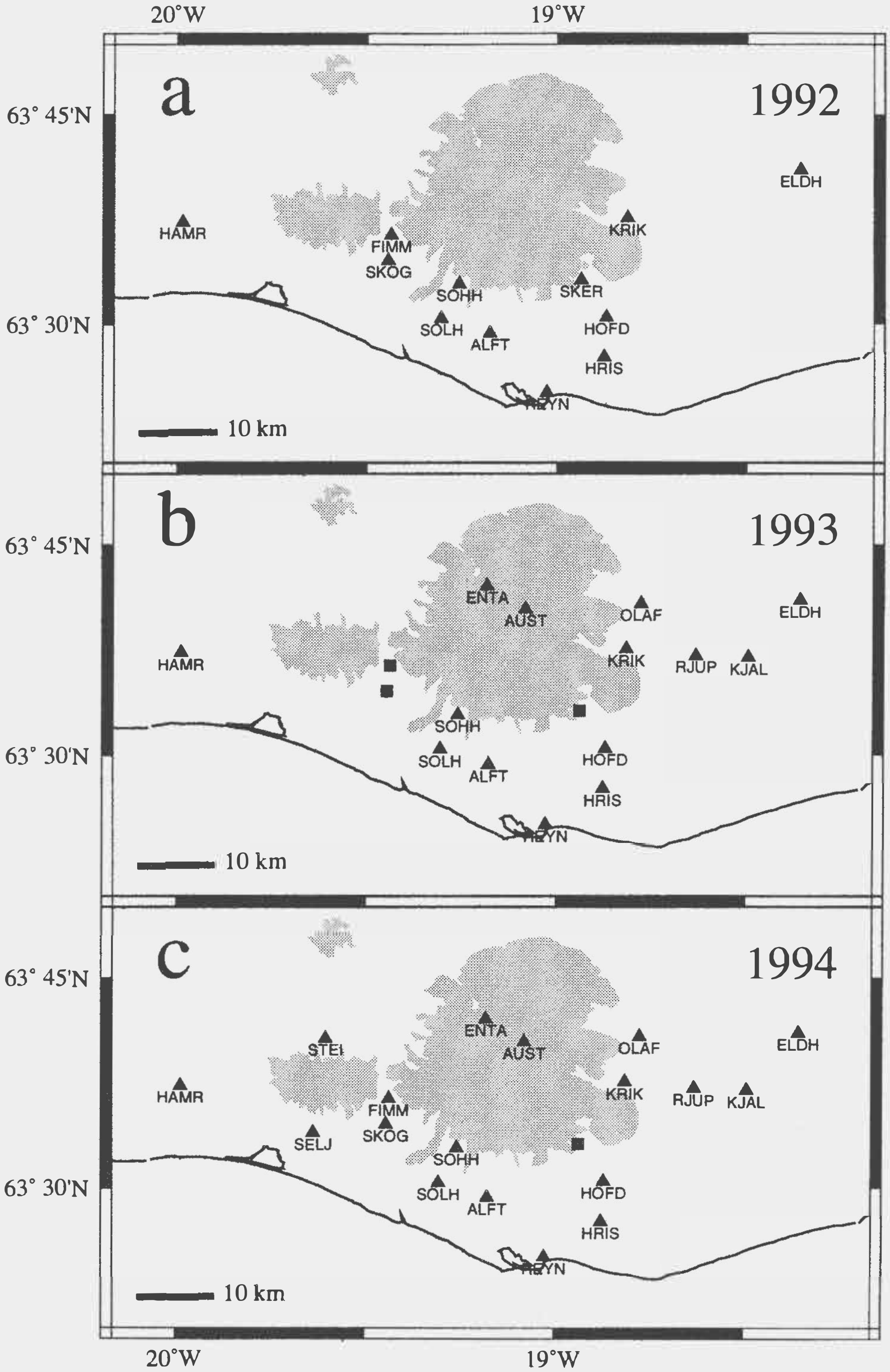

Figure 2.2: a) Points occupied in 1992. b) The whole network in 1993, three points were not measured that year (squares). c) The network was all measured in 1994, except one point (square).

The two new points, Steinsholt (STEI) and Seljavellir (SELJ) were established mainly because of the seismic unrest in Eyjafjallajökull in the spring of 1994. These points will play an important role for monitoring the volcano in the future. As a next step in the GPS-measurements around Eyjafjallajökull, it is important to add new points east of the benchmark Hamragarðar (HAMR) and on nunataks in the ice cap.

Under certain circumstances it can be difficult to access the two new points and a 4WD jeep is needed. To access the point Steinsholt (STEI), north of Eyjafjallajökull, one has to cross two glacier rivers on fords. To get close to the point, Seljavellir (SELJ), one has to drive up a very steep muddy track from the Seljavellir farm. On a wet day this is almost impossible.

The point Austmannsbunga (AUST), on one of the nunataks in Mýrdalsjökull glacier, shouldn't be measured before mid-June, because of snow. In 1994, in late May, we had to dig more than 1 m down to access this point. Other difficulties in 1994 were less important. We had minor problems to access the points Kötlukriki (KRIK), Ólafshaus (OLAF) and Sólheimaheiði (SOLH) because of snow on the track in late May. The benchmarks Skógaá (SKOG), Fimmvörðuháls (FIMM) and Sker (SKER) cannot be accessed until late summer.

The descriptions of the GPS-points in the network near Mýrdalsjökull and Eyjafjallajökull can partly be found in Einarsson (1993) and partly in Sigmundsson and Einarsson (1993b).

2.4 The Hekla Volcano Experiment

The Hekla Volcano has erupted for 17 times since the first historical eruption in 1104. Four eruptions have occurred in this century, in 1947, 1970, 1980-1 and in 1991. These last three eruptions in Hekla indicate that the volcano has entered a new phase of activity, with shorter repose periods and smaller eruptions. The main purpose of GPS-measurements around Hekla is to monitor the volcano and explore, under unique conditions, the eruption cycle of the volcano.

Systematic GPS-measurements around the Hekla volcano began in February 1991 just after an eruption started in January 17. Two measurements were conducted that year on a sparse network of only 7 points within a distance of 25 km from the mountain (Sigmundsson et al. 1992a). This network was measured for the third time in the summer of 1992.

In 1993, the network was heavily densified and 14 new points were added. The total network consisted then of 21 points which all were measured in July 1993.

The network was still densified in 1994 with two new points and it now consists of 23 control points, see Figure 2.3. A total of 19 points of the network were measured in 1994. Three of these four points which weren't occupied this year

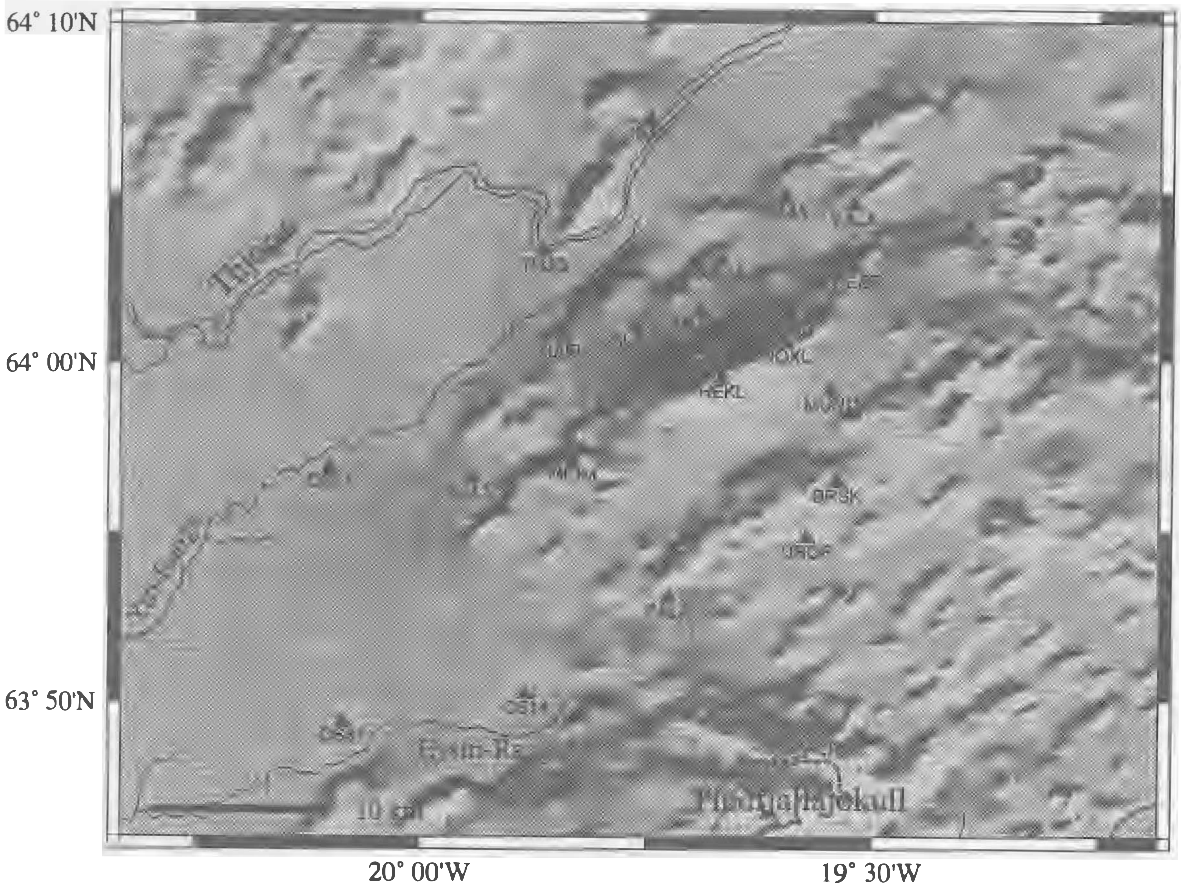

Figure 2.3: The Hekla volcano GPS-network. Most of the network was measured in 1994.

Abbreviation	*Name*	*Inscription*	*Approx. coord.*		
			Lat.	*Lon.*	*H*
ISAK	Ísakot	OS 7386	64 07 09 N	19 44 50 W	319
THJO	Þjófafoss	OS 7481	64 03 14 N	19 51 56 W	244
HAFU	Hafurshorn	NE 91 12	64 00 42 N	19 50 30 W	
MOHN	Móhnúkar	NE H7	64 01 30 N	19 41 28 W	
LITL	Litla Hekla	Steel rod	64 00 22 N	19 40 56 W	
SBJA	Suðurbjallar	NE 80 054	64 01 01 N	19 45 47 W	562
SKJA	Skjaldbreið	NE 80 047	64 04 50 N	19 35 57 W	454
VALA	Valahnúkur	RH 93 12	64 04 36 N	19 31 22 W	561
KROK	Krókagiljabrún	OS 1986 7418	64 03 58 N	19 23 45 W	585
HEKL**	Hekla	NE 94 12	63 59 31 N	19 40 02 W	1555
NOXL	Norðuröxl	Iron rod	64 00 34 N	19 35 49 W	1003
PALA	Pála	RH 93 11	63 53 05 N	19 43 32 W	
NBJA	Norðurbjallar	NE 80 058	64 02 58 N	19 40 10 W	
MUND	Mundafell	NE 80 056	63 59 08 N	19 32 51 W	
BRSK	Breiðaskard	NE 93 08	63 56 28 N	19 32 25 W	
DROP	Dropi	NE 93 07	63 54 50 N	19 34 24 W	
SELS	Selsund	NE 80 042	63 56 35 N	19 56 36 W	
RAUD**	Rauðkembingar	NE 93 29	64 01 38 N	19 35 28 W	
HEST	Hestalda	NE 80 046	64 02 45 N	19 31 12 W	
0S11*	Krókahraun	OS 7220	63 56 52 N	20 06 01 W	162
MIDM*	Miðmorgunshjúkur	NE 80 053	63 57 05 N	19 49 56 W	
0S14*	Skógshraun	OS 7365	63 50 14 N	19 52 56 W	340
0S61*	Keldur W	OS 7480	63 49 24 N	20 05 05 W	165

Table 2.2: GPS control points near the Hekla Volcano. Points marked by * were not measured in 1994. Points marked by ** were established in 1994. H is height above reference ellipsoid, in meters. Abbreviations of inscriptions: OS National Energy Authority, NE Nordic Volcanological Institute, RH The Science Institute of the University of Iceland.

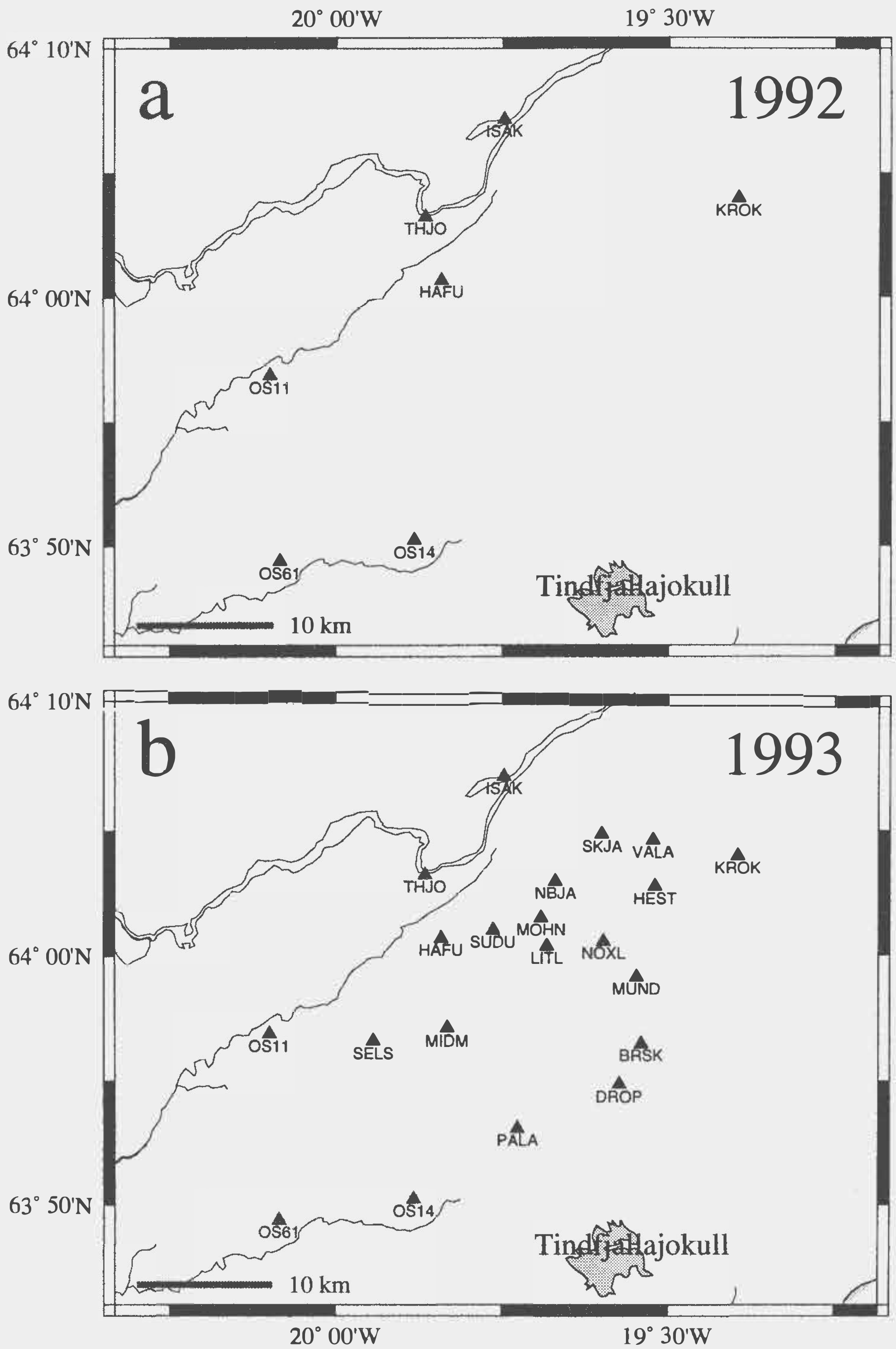

Figure 2.4: a) Points occupied in 1992. b) The network was densified and all measured in 1993.

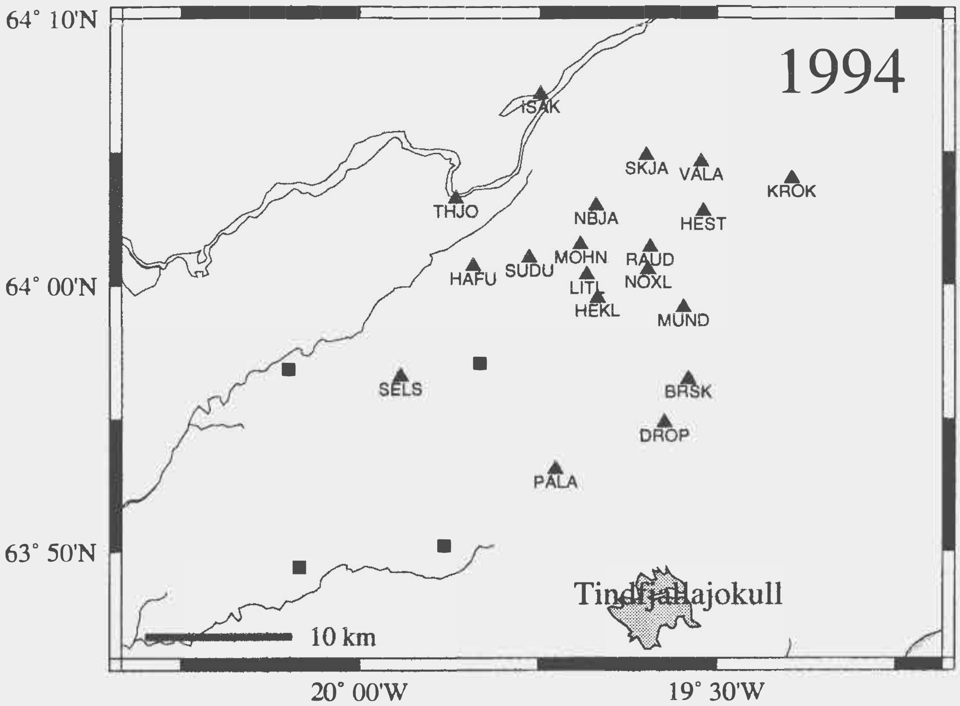

Figure 2.5: The GPS-measurements around the Hekla Volcano in 1994, four points of the network were not measured this year (squares).

are of less importance than most of the others because of long distance from the volcano, Krókahraun (0S11), Skógshraun (SKOG) and Keldur W (0S61). Considerable effort is needed to access the point Miðmorgunshjúkur (MIDM) and therefore it wasn't measured in 1994, see Table 2.2.

The GPS-points measured around the Hekla Volcano in 1992-94 are shown in Figures 2.4 and 2.5

The measurements in 1994 near the Hekla volcano and in the Eastern Volcanic Rift Zone were conducted in July 18-29 and from August 30 to September 17. The point Ísakot (ISAK) was, as usually, used as a reference station, partly because easy access and availability of AC power.

The new point on Rauðkembingar (RAUD) is a central point in a new tilt station close to the mountain. This point is usually easily accessible on a 4WD vehicle from July to September. The other new point was established on the highest peak of the volcano (HEKL) to constrain further possible subsidence or inflation of the mountain's peak and to measure the present height of the volcano. The height of Hekla has been varying on maps from 1450 to 1491 m.a.s.l., mainly because of changes during the recent eruptions. Our measurements show that the height was 1488.0 m.a.s.l. in September 1994. The point HEKL is difficult to access because it is on the top of the mountain. It is a 2-3 hours steep hike up to the top.

The GPS-point descriptions around Hekla volcano can be found in Sigmundsson and Einarsson (1993a) and in Einarsson (1993).

2.5 The Eastern Volcanic Rift Zone Experiment

The aim of this experiment is to measure relative movements in the Eastern Volcanic Rift Zone, in South Iceland, i.e. on the boundary between the Eurasian plate and the North American plate. Results of measurements in North Iceland have greatly expanded our knowledge about movements at divergent plate boundaries during and following a rifting episode (e.g. Gerke et al. 1978, Sigurðsson 1980, Möller et al. 1982, Kanngieser 1983, Tryggvason 1984, Björnsson 1985, Wendt et al. 1985 and Foulger et al. 1992). There haven't been big rifting episodes in South Iceland for more than hundred years, which gives an opportunity to explore the behavior of a similar divergent boundary, in a quiet phase.

The first measurements to explore the boundary movements in the Eastern Volcanic Rift Zone were made in 1967 when a 58.5 km long distance profile was established (Decker et al. 1971). The profile consists of 24 points with interval lengths of 1-5 km. This profile has been measured several times with geodimeter since 1967. In 1970, about half of the profile was measured, this was done few months after the Hekla eruption in 1970. A slight expansion was observed over the fissure swarm north of Hekla (Decker et al. 1971). The whole profile was measured in 1973, 1977 and 1986 and a little contraction was observed (Decker et al. 1976, Erlingsson and Einarsson 1995).

The first GPS-measurements in the Eastern Volcanic Rift Zone were made in 1986, a sparse network of 8 points was measured which was a part of a country-wide campaign (Foulger et al. 1993). The network was densified and measured again in 1989, 16 points, but results are available just for part of the points because of processing problems (Hackman 1991).

Nine points of the network in the Eastern Volcanic Rift Zone were measured in 1991 as a part of two different experiments. Four points were measured close to the Hekla Volcano to measure the post-eruption subsidence of the volcano. The Ísakot (ISAK) control point was used as a reference station. Five points were also measured SE of the Vatnajökull ice-cap to detect glacio-isostatic movements. Two of them were measured for the first time in 1991, Breiðbakur (BREI) and Langisjór N (NLAN), see Figure 2.8a. Results are missing for one of these five points (3371), because of unexplained processing problems (Sigmundsson 1992). The point Langisjór S (SLAN) was used as a reference station for this survey.

A total of 8 points of the network in the Eastern Volcanic Rift Zone were

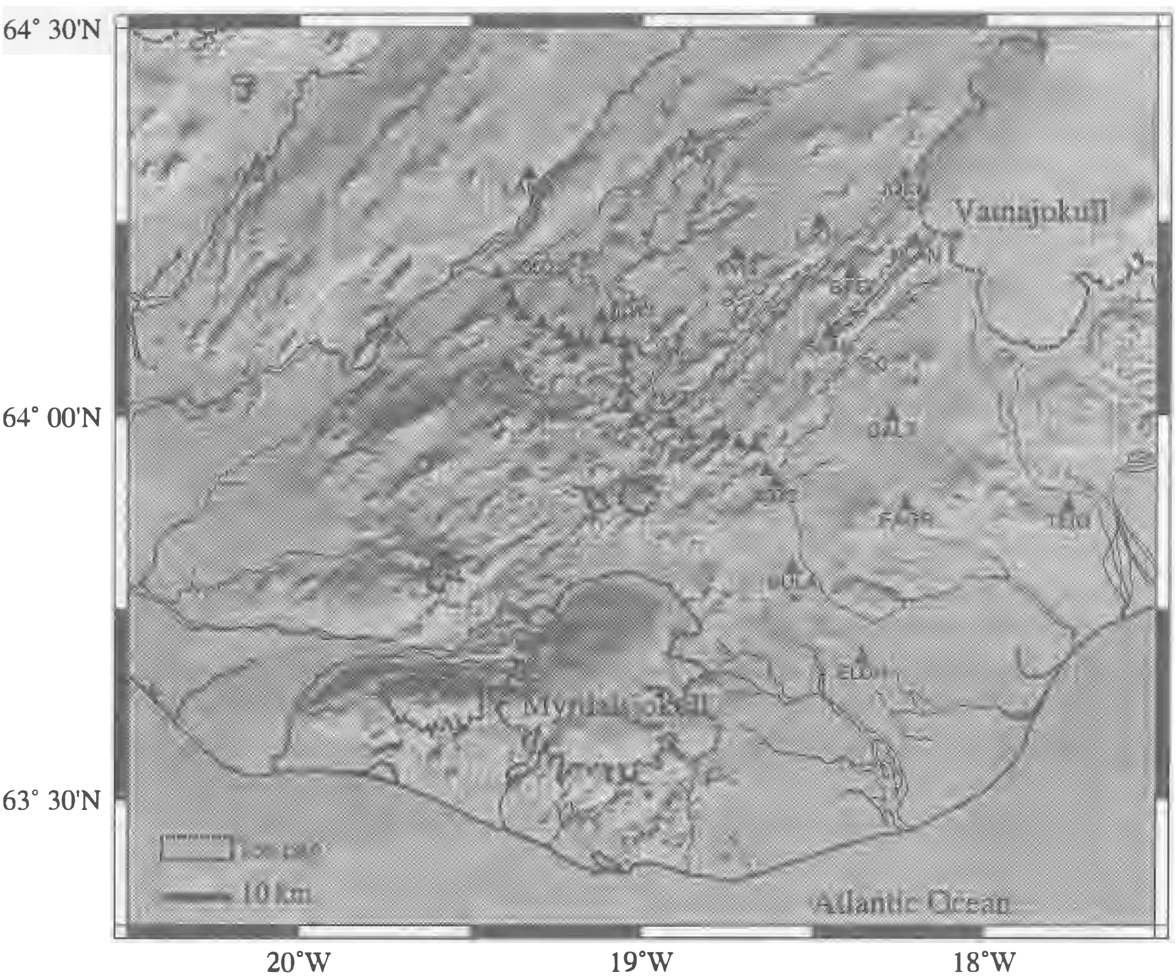

Figure 2.6: GPS points in the Eastern Volcanic Rift Zone network, the whole network was measured in 1994.

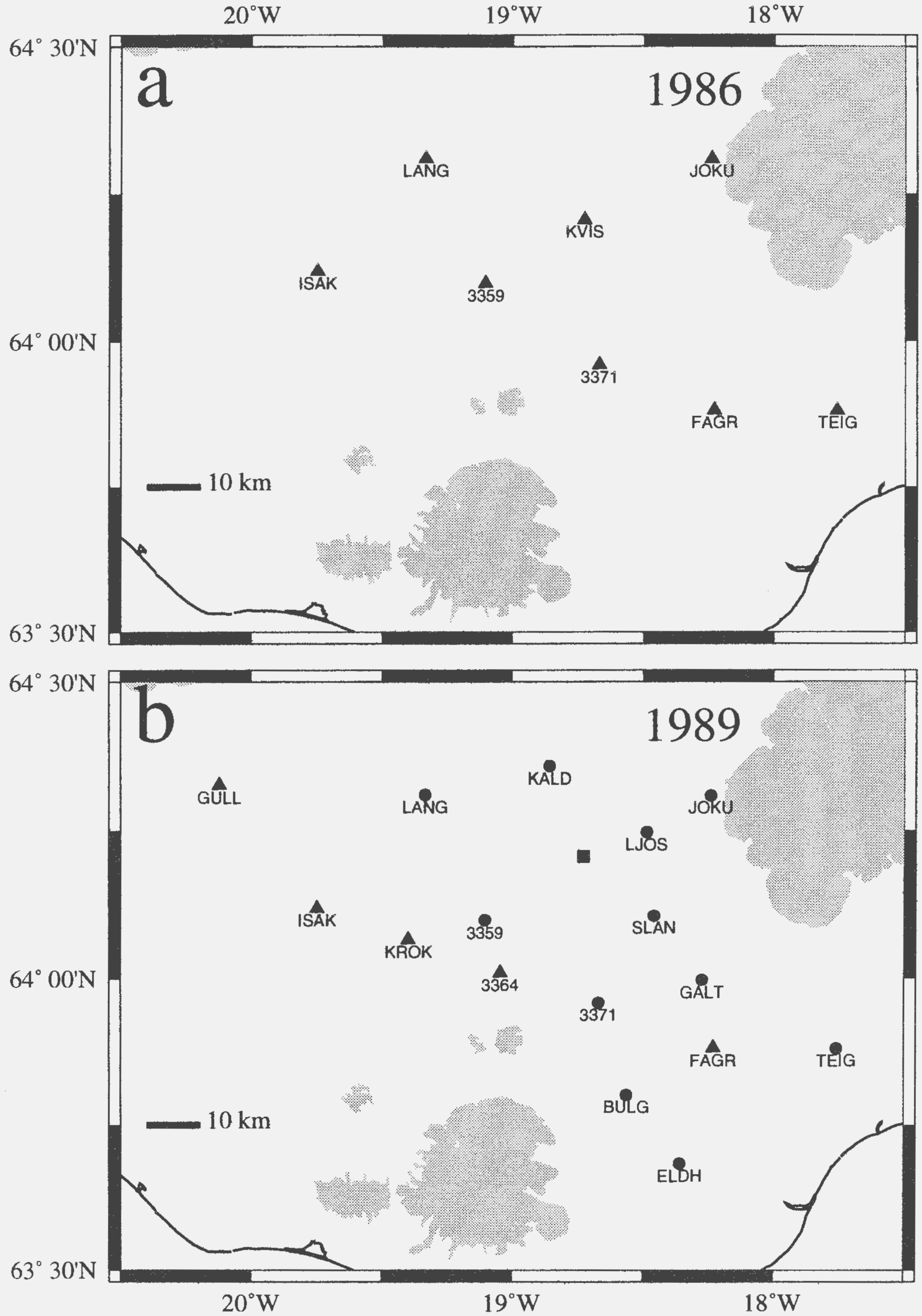

Figure 2.7: a) GPS points in the Eastern Volcanic Rift Zone measured in 1986. b) Points measured in 1989. No results exist for many of occupied points because of processing problems (dots). One point of the network from 1986 was not measured this year (square).

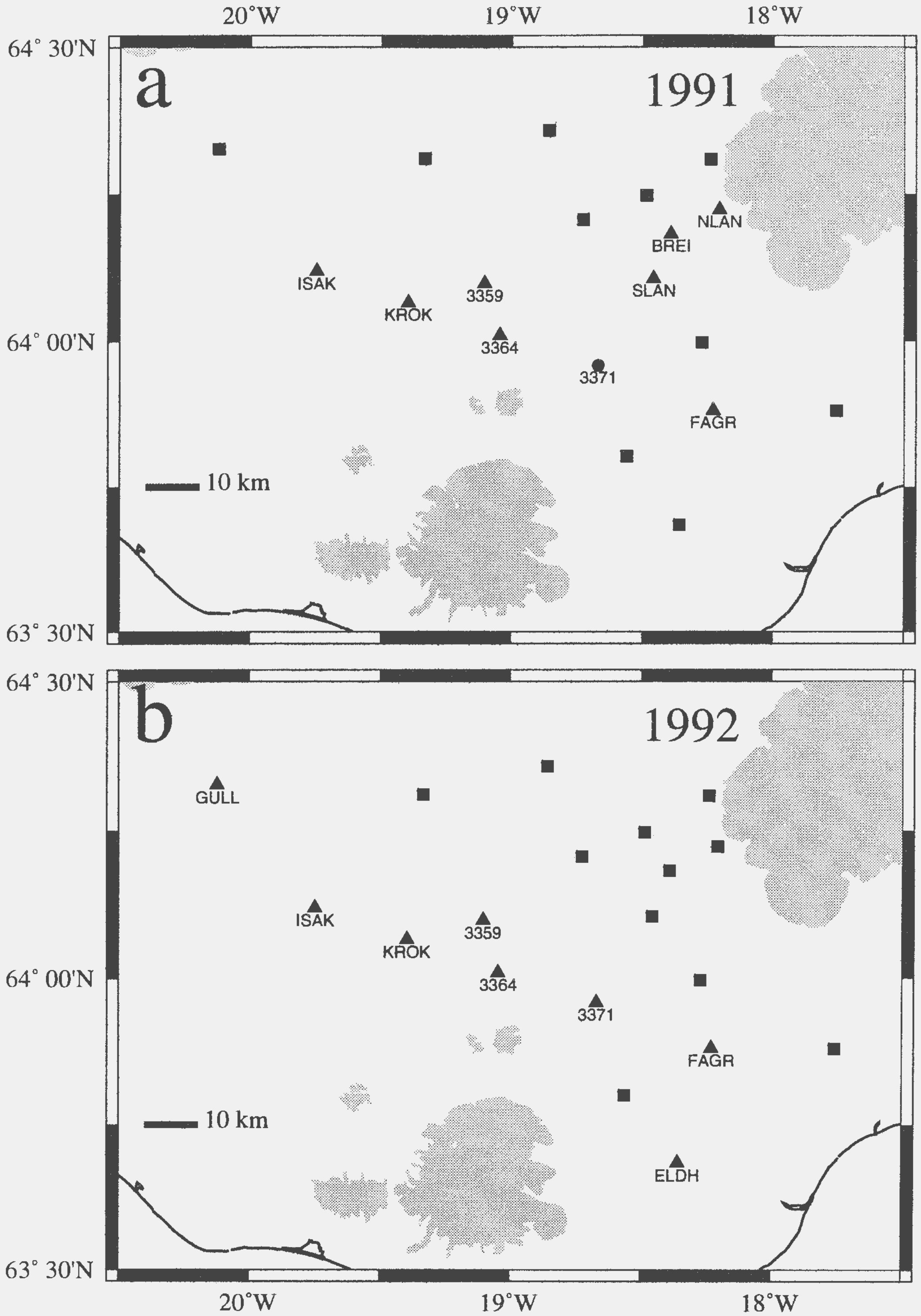

Figure 2.8: a) GPS points in the Eastern Volcanic Rift Zone measured in 1991. b) Points measured in 1992. Squares indicate points of the network that weren't occupied these years.

Abbreviation	*Name*	*Inscription*	*Approx. coord.*		
			Lat.	*Lon.*	*H*
ISAK*	Ísakot	OS 7386	64 07 10 N	19 44 50 W	319
3359	Bjallavað	D. 3359	64 05 56 N	19 06 15 W	604
3364	Frostastaðaháls	D. 3364	64 00 36 N	19 02 40 W	714
3366	Kýlingar	D. 3366	63 59 26 N	18 55 06 W	704
3357	Litla Melfell	D. 3357	64 05 51 N	19 10 45 W	615
3367	Jökuldalir	D. 3367	63 58 34 N	18 51 36 W	780
0D17	Sigöldulína	0D 17	64 07 34 N	19 07 12 W	598
LJOS	Ljósufjöll E	OS 7484	64 14 54 N	18 29 08 W	724
JOKU	Jökulheimar	OS 7383	64 18 34 N	18 14 24 W	740
KVIS	Kvíslarfell	(OS 5145)	64 12 25 N	18 43 30 W	757
KALD	Kaldakvísl	OS 1989 7491	64 21 31 N	18 51 26 W	606
3350	Hald	D. 3350	64 11 00 N	19 25 09 W	374
LANG	Langahlíð	OS 2069	64 18 38 N	19 19 58 W	665
3351	Búrfellshraun	D. 3351	64 09 50 N	19 23 41 W	437
3352	Taglgígahraun	D. 3352	64 08 41 N	19 22 42 W	469
3358	Dyngjuskarð	D. 3358	64 05 34 N	19 09 18 W	616
3353	Heklutögl	D. 3353	64 07 48 N	19 21 06 W	498
3361	Hnausar	D. 3361	64 04 34 N	19 02 56 W	635
3360	Tungnaá	D. 3360	64 05 35 N	19 03 17 W	631
FAGR	Fagrifoss	OS 7376	63 52 55 N	18 13 47 W	480
GALT	Galti	OS 7485	63 59 52 N	18 16 21 W	678
ELDH*	Eldhraun	OS 5847	63 41 05 N	18 21 26 W	146
TEIG	Teigingalækur	OS 5819	63 52 53 N	17 45 31 W	106
BULA**	Búland	NE 94 11	63 48 09 N	18 33 34 W	296
BULG	Búland G	OS 5834	63 48 08 N	18 33 37 W	296
3373	Skaftá	D. 3373	63 54 47 N	18 36 39 W	503
3372	N Ófæra	D. 3372	63 55 43 N	18 38 05 W	467
3371	Herðubreiðarháls	D. 3371	63 57 34 N	18 40 06 W	772
3368	Steinsgil	D. 3368	63 58 25 N	18 47 13 W	757
3369	Tindafjöll	D. 3369	63 58 31 N	18 45 52 W	776
3365	Kýlingaskarð	D. 3365	63 59 32 N	19 01 10 W	749
3363	Tjörvafell	D. 3363	64 02 03 N	19 03 00 W	664
3362	Bláhylur	D. 3362	64 03 23 N	19 03 10 W	688
3356	Laufdalsvatn	D. 3356	64 05 37 N	19 12 35 W	590
BREI	Breiðbakur	FM 354	64 10 58 N	18 23 28 W	883
NLAN	Langisjór N	RH 91 02	64 13 27 N	18 12 23 W	732
SLAN	Langisjór S	FM 546	64 06 23 N	18 27 23 W	747
3370	Skuggafjöll	D. 3370	63 57 47 N	18 43 08 W	741
KROK*	Krókagiljabrún	OS 1986 7418	64 03 58 N	19 23 46 W	585
3355	Dyngjur	D. 3355	64 06 21 N	19 14 07 W	585
3354	Dyngjuhorn	D. 3354	64 07 06 N	19 17 42 W	523
GULL	Gullfoss	OS 5469	64 19 39 N	20 07 18 W	277

Table 2.3: GPS control points in the network of the Eastern Volcanic Rift Zone. Points marked by * are also part of either the Hekla volcano network or the Mýrdalsjökull network. The point marked by ** is new. H is height above reference ellipsoid, in meters. Abbreviations of inscriptions: D. Dartmouth College, New Hampshire, OS National Energy Authority, NE Nordic Volcanological Institute, RH The Science Institute of the University of Iceland.

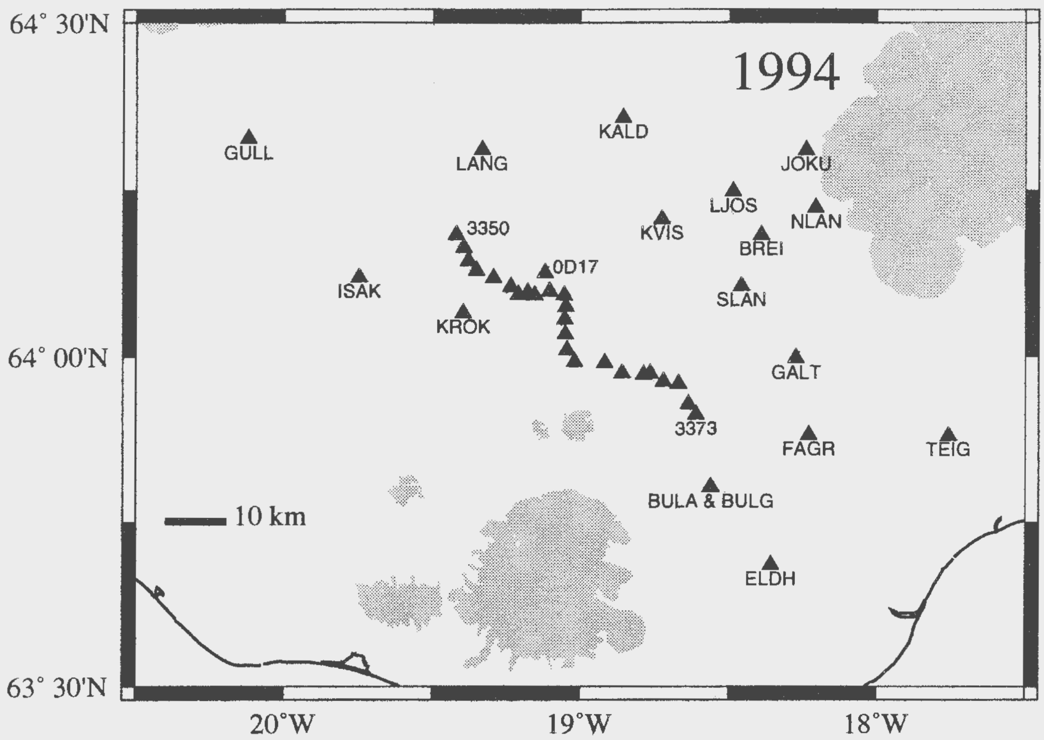

Figure 2.9: GPS stations in the Eastern Volcanic Rift Zone measured in 1994.

remeasured in 1992 as a part of a campaign in South Iceland (Sigmundsson et al. 1992b and 1995).

In 1994 the largest GPS-campaign in the Eastern Volcanic Rift Zone so far was conducted, 42 points were measured. The whole network from 1986, 1989 and 1991 was remeasured, 19 points. The distance profile was now measured with GPS receivers for the first time, 24 points (three of them are also in the previous GPS-network, 3359, 3364 and 3371). One point from 1973, just beside the profile (0D17), was also measured in 1994. One new benchmark was established, Búland (BULA). The new point is just about 50 m from the old Búland point (BULG), which was considered to be too close to the track of Nyrðra-Fjallabak.

The 1986-1994 GPS points measured in the Eastern Volcanic Rift Zone are shown in Figures 2.7, 2.8 and 2.9.

The 1994 measurements were conducted from July 18 to July 29 and from August 30 to September 17. The baseline Ísakot(ISAK)-Gullfoss(GULL) was measured from October 31 to November 1. The Ísakot control point was used as a reference station during the whole campaign. In addition to this, four points were measured in Hvalfjörður, about 20 km north of Reykjavík, on November 3-5. Árnagarður (ARNA), a control point in Reykjavík was used as a reference station. Three of these points have been used since 1967 to

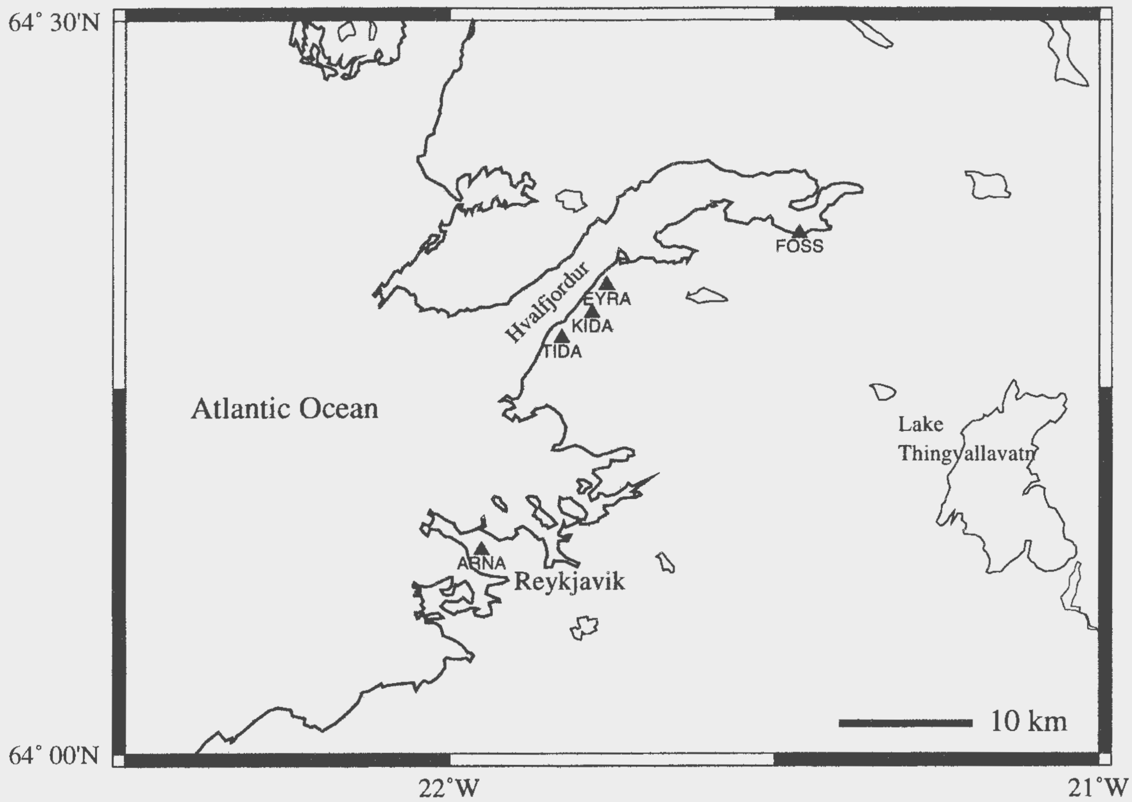

Figure 2.10: The network in Hvalfjörður measured in November 3-4, 1994.

measure scale factor differences between geodimeter instruments, since these points are considered to be located in a stable area, from a tectonic point of view, see Figure 2.10.

Descriptions for all the points in the network can be found in Einarsson (1993), except the profile points, where one has to contact P. Einarsson at the Science Institute of the University of Iceland to get descriptions.

Chapter 3

Processing of Data from the Eastern Volcanic Rift Zone

3.1 General Remarks

The data from the Eastern Volcanic Rift Zone were analysed with the Bernese GPS software, version 3.5. Three coordinate results were produced for each point using different information and methods:

1. Station coordinate estimation using broadcast orbit information. The results are in the WGS-84 (World Geodetic System 84) reference frame.

2. Station coordinate estimation using precise IGS (International GPS Service for Geodynamics) orbit information, this gives the results in ITRF-92 (the 1992 IERS Terrestrial Reference Frame, IERS = International Earth Rotation Service).

3. Station coordinate estimation using precise IGS orbit information and station specific estimation of tropospheric zenith delay.

Data from 46 stations were processed (including the reference station), 42 stations are within the Eastern Volcanic Rift Zone network but the extra 4 are in the Hekla Volcano network. The data from Hvalfjörður (5 stations) were processed independently and just with the second method, described above.

The major processing steps are described below. To execute these steps, we used series of batch programs from UNAVCO which automate the Bernese software (UNAVCO 1994).

3.2 Data Transfer

In the beginning we transferred the raw data from the Trimble receivers into RINEX format (Receiver Independent Exchange Format, Gurtner et al. 1989).

We transferred the navigation messages and the observation data from RINEX format to Bernese (version 3) format (programs RXNBV3 and RXOBV3). This gave three types of files, Bernese broadcast files, phase and code observation files.

3.3 Orbit Processing

The broadcast ephemerides were checked in the beginning for any obviously wrong messages about the satellite orbits or clock parameters (program BRDTST).

The broadcast ephemeris and the precise IGS orbits are in earth centered, earth fixed coordinate system which rotates with the earth. The orbit information were transformed to an inertial reference frame by the program BRDTAB (or PRETAB, in case of precise IGS orbits) which creates tabular orbit files.

The next step in the orbit processing was to create standard orbits for the Bernese software, which is done by taking the series of satellite positions as observations (tabular orbits) and generate satellite arcs through numerical integration (program DEFSTD). We generated one arc per satellite per day and estimated 8 orbit parameters for each arc. Six parameters define uniquely the initial conditions (position and velocity) of a satellite at start time of the arc. Two dynamical parameters were also estimated, p_0, a direct solar radiation pressure parameter and p_2, y-bias.

At the end of orbit processing, we had two sets of orbit arcs files and radiation pressure parameters files for each day, one made from precise IGS orbit informations and another from broadcast ephemeris.

3.4 Data Preprocessing

As a first step in processing the observation data we checked the code observations (program CODCHK). The program marks outliers in the data using the assumption that code observations may be represented as a smooth function of time (Rothacher et al. 1993). Preliminary station coordinates were calculated from checked code observations (program CODSPP) and receiver clock corrections were estimated for each epoch since polynomial clock corrections are not suitable for Trimble receiver clocks. The preliminary coordinates were held fixed through the clock corrections.

Phase single differences were made from phase file pairs (program SNGDIF). This was followed by outlier rejection and cycle slip correction of the single difference files (program MAUPRP). Further rejections and corrections were manually made with GT, an editing program from UNAVCO, where one can have residual double differences displayed through time.

Noise and frequent cycle slips were problematic in a few sessions of the data, but very few sessions were completely discarded. These problems were most prominent around and after midnight which correlates with the frequency of unstable behaviour of the ionosphere in auroral areas. High heterogeneity of the ionosphere in space and time in Iceland is a potential major error source in Icelandic GPS data (Sigmundsson 1992).

Cleaned of cycle slips and outliers, the usable data set was now ready for further processing; coordinate estimation and ambiguity resolution.

3.5 Parameter Estimation

The final solution was made from three steps, each step was executed for one day of the data set.

1. Station coordinates estimation using the ionospheric free (L3) linear combination without fixing ambiguities.

2. Wide lane (L5) linear combination ambiguities were resolved by keeping estimated coordinates from step 1 fixed.

3. Final station coordinates solution using ionospheric free (L3) linear combination, introducing the fixed wide lane (L5) ambiguities from step 2.

These three steps were completed for both the broadcast orbit and precise IGS orbit information. An additional solution was also created using precise IGS orbits, estimating both the coordinates and hourly station specific tropospheric zenith delay parameters.

The effect from the troposphere on the GPS-signal can be divided in two, the dry and wet tropospheric delay. Even though the dry part is about 90% of the delay, the wet part is the critical one, because it is relatively easy to model the dry effect (pressure). The wet effect varies in space and time and can cause bad results. The tropospheric delay is estimated mainly by two different methods:

- Modeling the delay (without GPS data), by using standard tropospheric refraction models (e.g. Saastamoinen 1972 and Hopfield 1971). One can also add surface meteorological data and WVR (water vapor radiation) data to this modeling.

- Estimating the delay by using a standard tropospheric refraction model as a priori information, and then estimate station specific delay parameters.

We calculated two coordinate solutions using the former method, one for each type of orbit information. No meteorological or WVR data were collected. Because of the size of the Eastern Volcanic Rift Zone network (approx. 125x75 km), we also produced the third coordinate result using the latter tropospheric delay method, described above.

Chapter 4

Results

4.1 Formal Uncertainties

The formal uncertainties, calculated by the Bernese software, indicate the phase data scatter, but do not include systematic errors and are found to be too optimistic estimate of the true uncertainties. This underestimate of the data uncertainties may be caused by unmodeled systematic effects (such as multipath effects) or mismodeled parameters (such as poor orbits) (UNAVCO 1994). The problem is enhanced by high data sampling which does not contribute to reducing systematic effects, but does reduce the formal errors (UNAVCO 1994).

The average Bernese formal uncertainties of the coordinate solutions from the Eastern Volcanic Rift Zone and Hvalfjörður are shown in Table 4.1. The formal errors are at sub-millimeter level, except the height and Z components of the precise orbits and tropospheric parameters solution.

4.2 Repeatability and Scaling Factors

Session-to-session repeatability is a common estimate of real uncertainties of GPS results. Repeatability R of a vector baseline component (east, north or vertical) is defined as the RMS scatter about the weighted mean (Dixon 1991):

$$R \equiv \left(\frac{\frac{n}{n-1} \cdot \sum_{i=1}^{n} \frac{(c_i - \langle c \rangle)^2}{\sigma_i^2}}{\sum_{i=1}^{n} \frac{1}{\sigma_i^2}} \right)^{1/2} \tag{4.1}$$

	Coordinate result			
Component	*Broadcast orbits*	*Precise orbits*	*P. orbits & trop. par.*	*Hvalfjörður results*
Number of coordinates	45	45	45	4
Number of solutions	87	86	88	8
Latitude (mm)	0.22	0.20	0.15	0.31
Longitude (mm)	0.17	0.16	0.13	0.25
Height (mm)	0.51	0.47	1.29	0.73
Length (mm)	0.18	0.16	0.16	0.29
X (mm)	0.24	0.22	0.57	0.33
Y (mm)	0.19	0.17	0.24	0.25
Z (mm)	0.49	0.46	1.16	0.71
Average (mm)	0.29	0.26	0.53	0.41

Table 4.1: The average of Bernese formal uncertainties of ellipsoidal coordinates, length and geocentric coordinates for all the three different coordinate results and the Hvalfjörður results.

where n is the number of component estimations for each station, c_i is one estimate of the component, and $\langle c \rangle$ is its weighted average:

$$\langle c \rangle = \frac{\sum_i \frac{c_i}{\sigma_i}}{\sum_i \frac{1}{\sigma_i}} \tag{4.2}$$

The repeatability can be a good description of the true uncertainties of GPS results, particularly when there are many independent coordinate solutions from each site.

As mentioned above, we calculated final network coordinate solution for each day in the dataset, and because we moved the receivers during the day and occupied each benchmark just once, this gave just two independent coordinate solutions for each point. This, of course, limits the significance of calculated statistical repeatability.

Average campaign repeatabilities for ellipsoidal coordinates, baseline lengths and geocentric coordinates are in Table 4.2 for the three coordinate sets and the Hvalfjörður results. The repeatability is significantly higher for the broadcast orbits solution than for precise orbits solutions, as expected. Station specific tropospheric zenith delay parameter estimation slightly decreases the repeatabilities, especially in the height component. Repeatability as a function of baseline length is plotted for all the coordinate solutions in Figures A.1-A.4.

We calculated a scaling factor to see the difference between the Bernese

	Coordinate result			
Component	*Broadcast orbits*	*Precise orbits*	*P. orbits & trop. par.*	*Hvalfjörður results*
Latitude (mm)	3.03	2.06	2.08	3.53
Longitude (mm)	3.92	2.17	1.79	1.60
Height (mm)	10.74	9.72	8.68	7.11
Length (mm)	3.77	2.29	1.99	3.35
X (mm)	4.76	4.02	3.98	3.50
Y (mm)	3.92	2.28	1.61	2.99
Z (mm)	9.92	9.03	7.89	6.75
Average (mm)	5.72	4.51	4.00	4.12
Scaling factor	22.7	18.3	11.2	12.1

Table 4.2: Campaign repeatabilities (of ellipsoidal coordinates, baseline lengths and geocentric coordinates) and scaling factors for the three coordinate solutions and the Hvalfjörður results.

formal uncertainties and the uncertainties indicated by comparison of independent sessions. The scaling factor simply indicates of what factor the formal uncertainties (σ_i) are different from those indicated by session to session scatter. First, the χ^2 is calculated for each of the seven components, north, east, height, length, X, Y and Z:

$$\chi^2 = \sum_{i=1}^{n} \frac{(c_i - \langle c \rangle)^2}{\sigma_i^2} \tag{4.3}$$

where n is the number of independent coordinate estimations and $\langle c \rangle$ is their corresponding weighted mean, see Equation 4.2. Then the scaling factor is adjusted to normalize the average of the seven $\chi^2 s$ to 1. The uncertainties indicated by session to session scatter are about one magnitude bigger than the formal uncertainties, as one can see from the scaling factors in Table 4.2. The reason for low scaling factor for the precise orbits and tropospheric parameters solution is partly because of high formal error of the height component and partly because of little session to session scatter of this solution. On the other hand, relatively shorter baselines are the reason for the low scaling factor of the Hvalfjörður solution. The average baseline length is about 23 km in the Hvalfjörður solution, but 43 km in the other solutions.

	Coordinate result			
Component	*Broadcast orbits*	*Precise orbits*	*P. orbits & Trop. par.*	*Hvalfjörður results*
Latitude (mm)	4.33	3.29	2.18	3.00
Longitude (mm)	3.42	2.56	1.62	2.25
Height (mm)	10.02	7.76	13.78	7.25
Average (mm)	5.92	4.54	5.86	4.17

Table 4.3: Average of scaled sigmas of ellipsoidal coordinates for the three coordinate solutions and the Hvalfjörður results based on DYNAP.

4.3 Scaled Sigmas by DYNAP

The program DYNAP (Dynamic Adjustment Program) from the National Geodetic Survey, USA, was used to compute a weighted network solution for all the dataset and produce baseline statistics. First, full coordinate correlation matrices were calculated for each measurement session from the Bernese covariances and uncertainties:

$$\rho_{ij} = \frac{cov_{ij}}{\sigma_i \sigma_j} \tag{4.4}$$

Then DYNAP was used to compute a weighted least squares network adjusted solution which includes full correlations in the weighting. Finally, we had then scaled sigmas for our coordinate solution, i.e. the input Bernese formal errors scaled by the variance of unit weight calculated by DYNAP. The program just calculates scaled sigmas for ellipsoidal components (latitude, longitude, height) but not for geocentric components (X, Y, Z) or baseline length.

The averages of scaled sigmas from DYNAP are shown in Table 4.3. The broadcast orbits solution has about 1 mm higher sigma in the horizontal components than the precise orbits solution and about 2 mm higher than the precise orbits solution with tropospheric parameters. The average scaled sigma, of the height component, for the precise orbits solution is about 2 mm lower than for the broadcast orbits solution, but the precise orbits solution, including tropospheric parameters, has average scaled sigma far above the other two solutions. This is due to high Bernese formal errors of the height component for this coordinate solution.

Scaled sigmas of each coordinate solution for the north, east, and height component are plotted for every station on Figures 4.1-4.7.

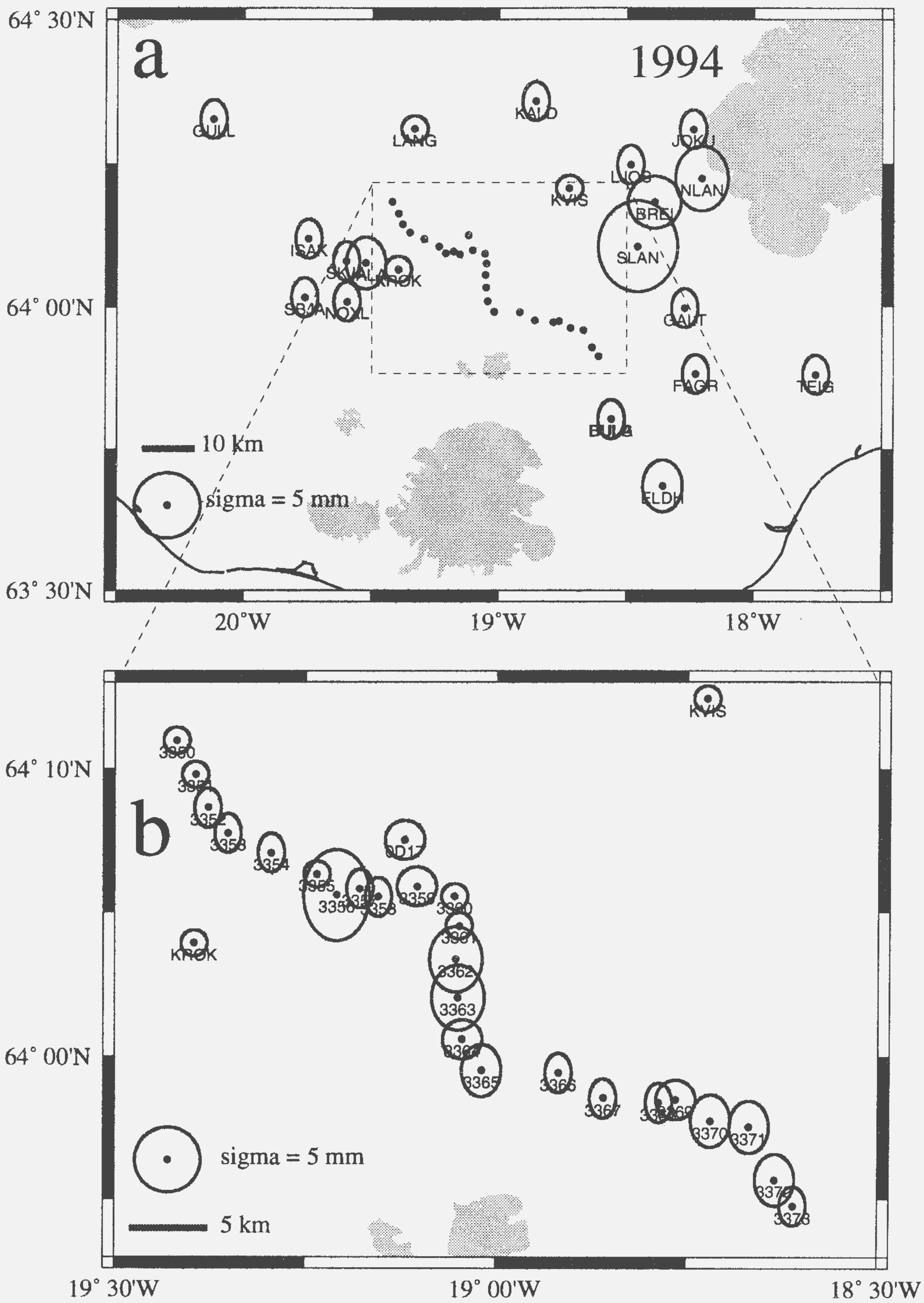

Figure 4.1: Scaled sigmas of the broadcast orbits coordinate solution of measured stations, horizontal components. Figure b is a plot of the distance profile in detail.

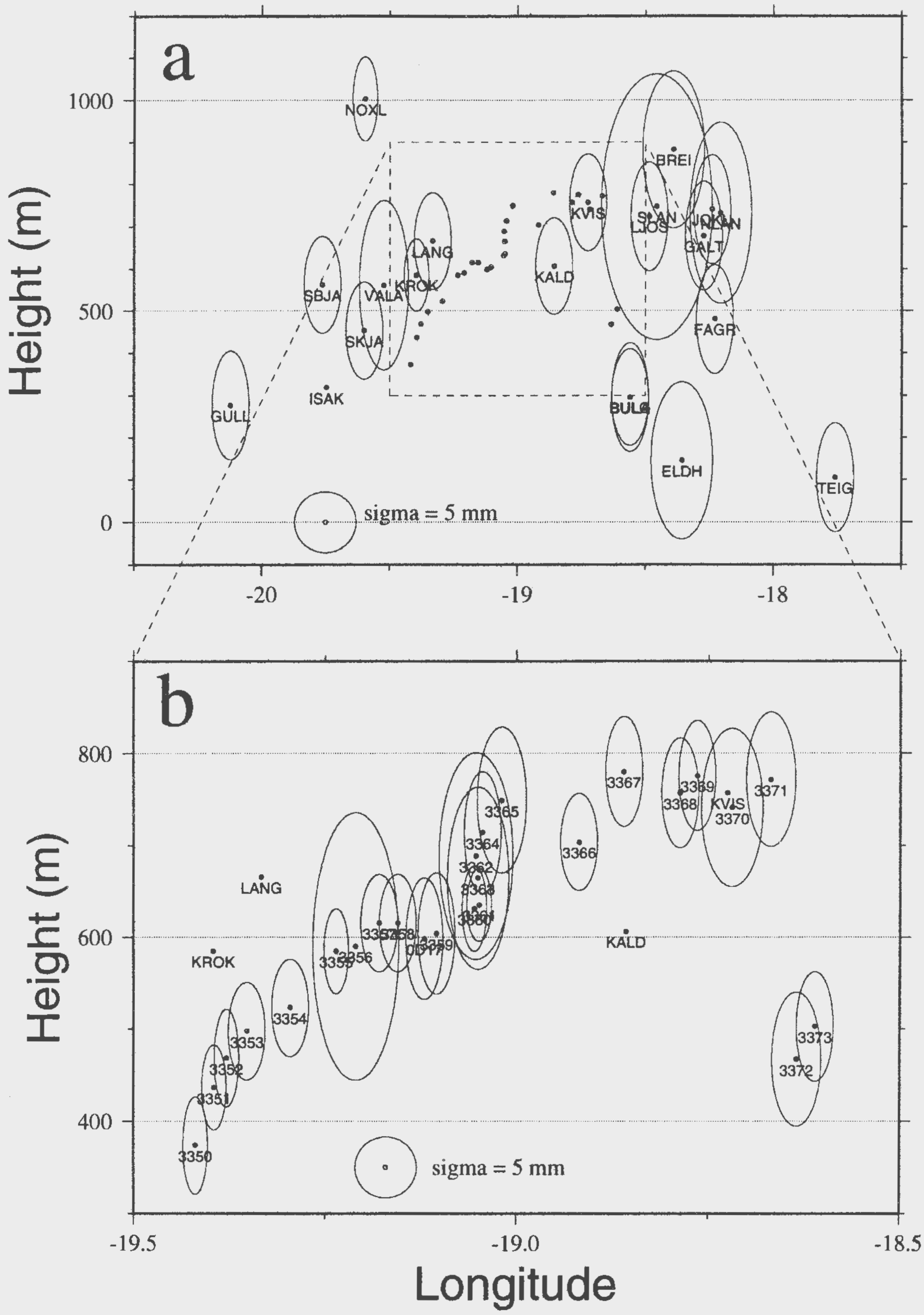

Figure 4.2: Scaled sigmas of the broadcast orbits coordinate solution. Height of station above reference ellipsoid is on the y-axis but longitude on the x-axis. The ellipses indicate scaled sigmas in height and east components.

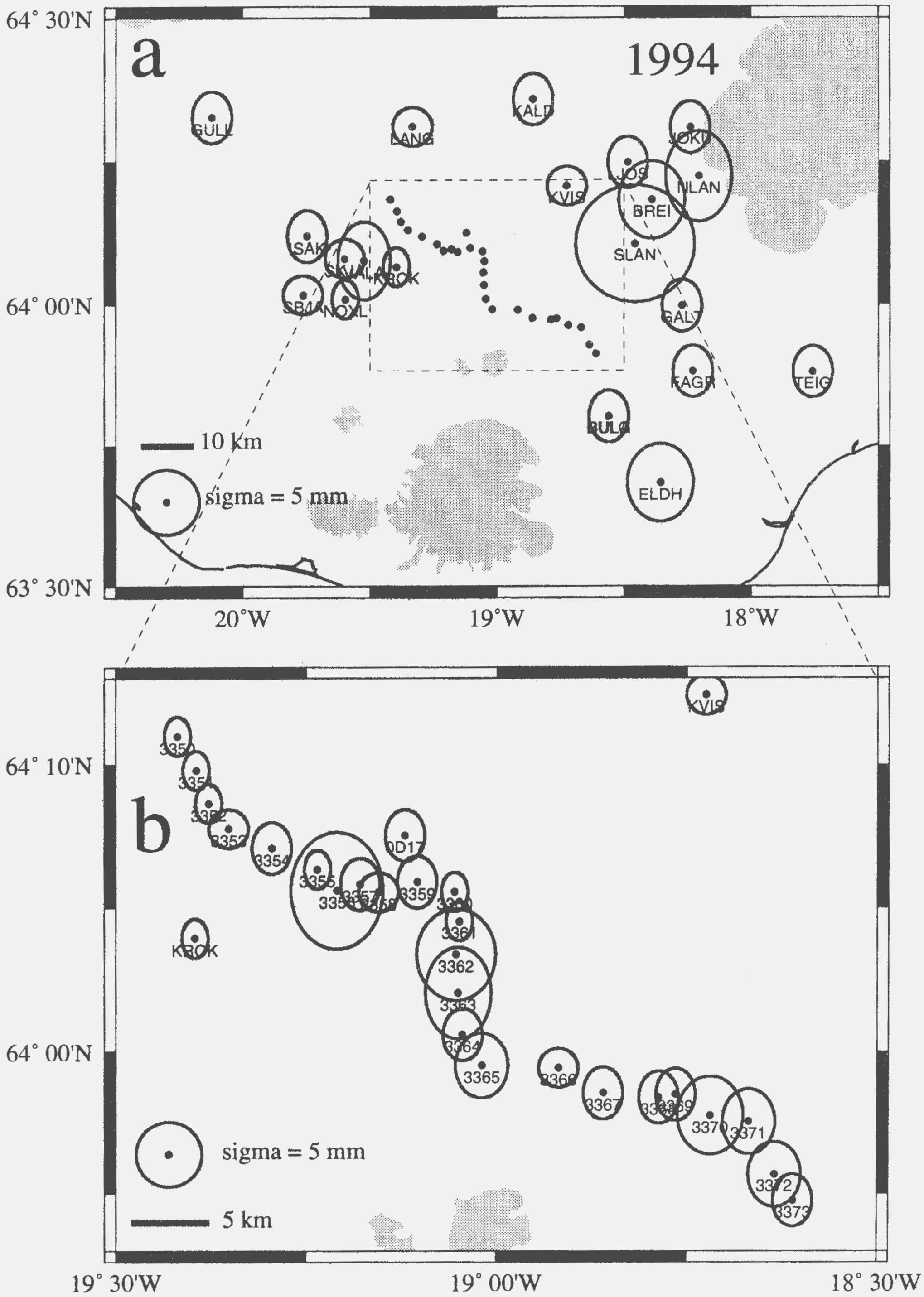

Figure 4.3: Same as Figure 4.1, except for sigmas of the precise orbits coordinate solution.

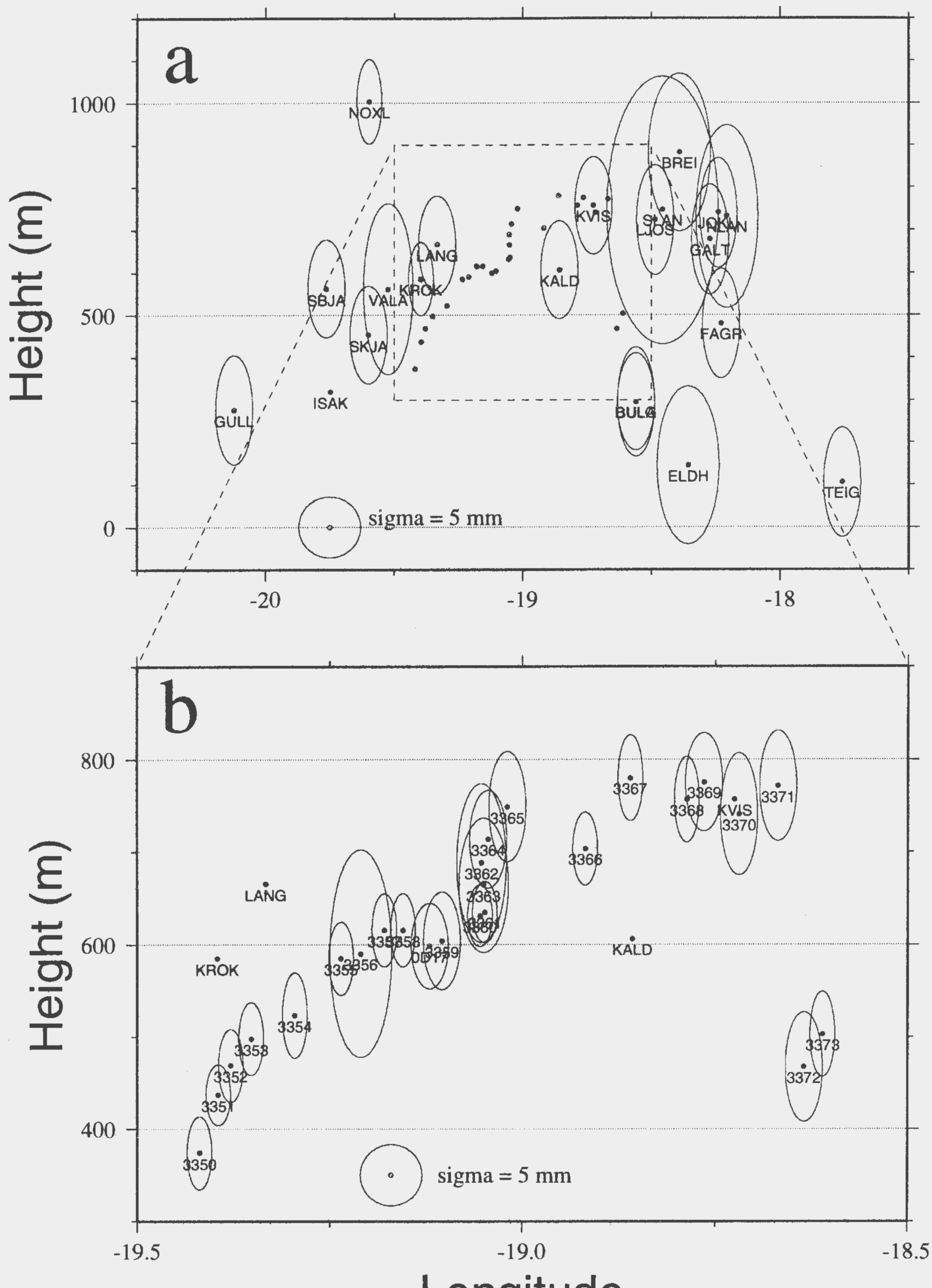

Figure 4.4: Same as Figure 4.2, except for sigmas of the precise orbits coordinate solution.

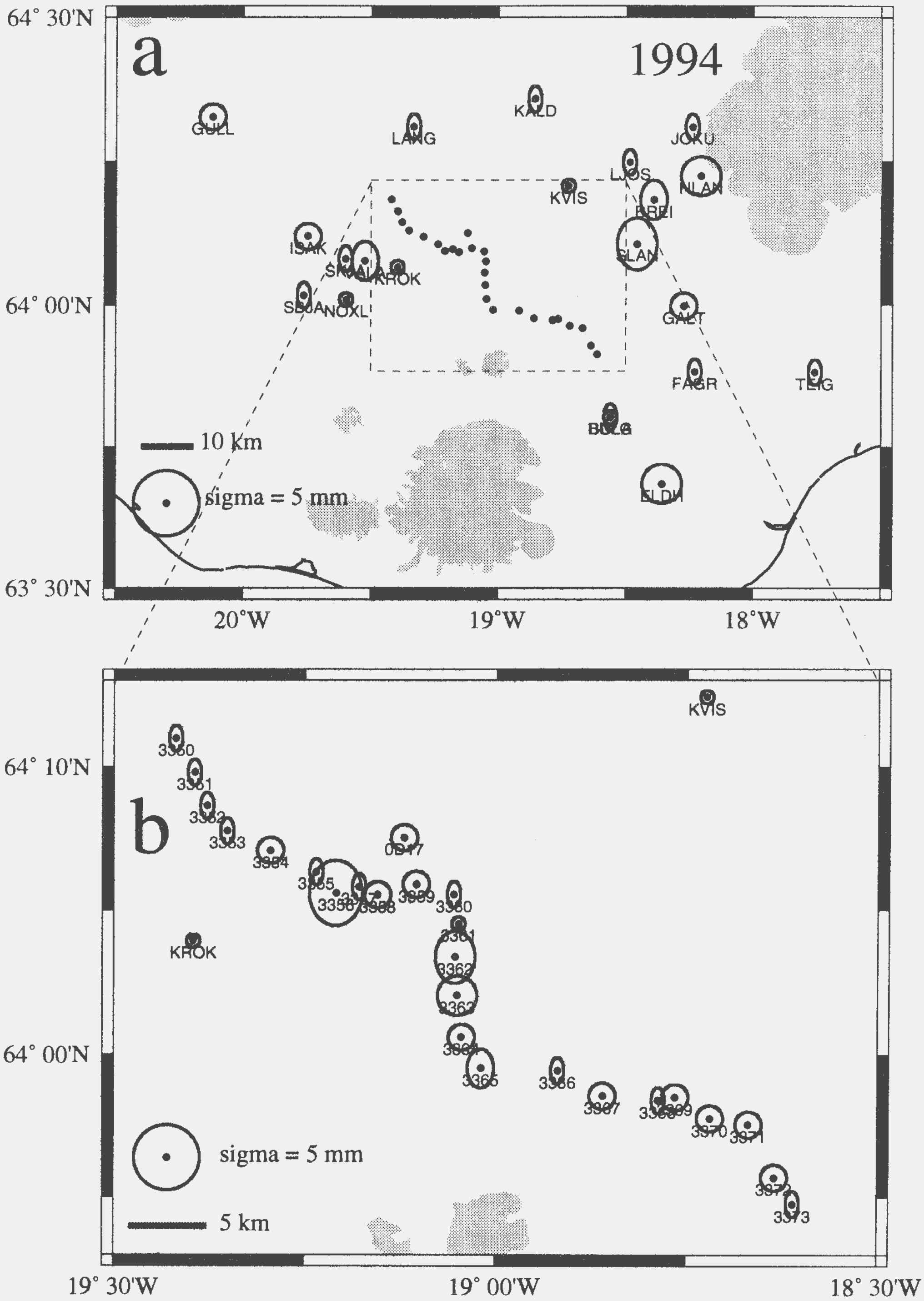

Figure 4.5: Same as Figure 4.1, except for sigmas of the precise orbits and tropospheric parameters coordinate solution.

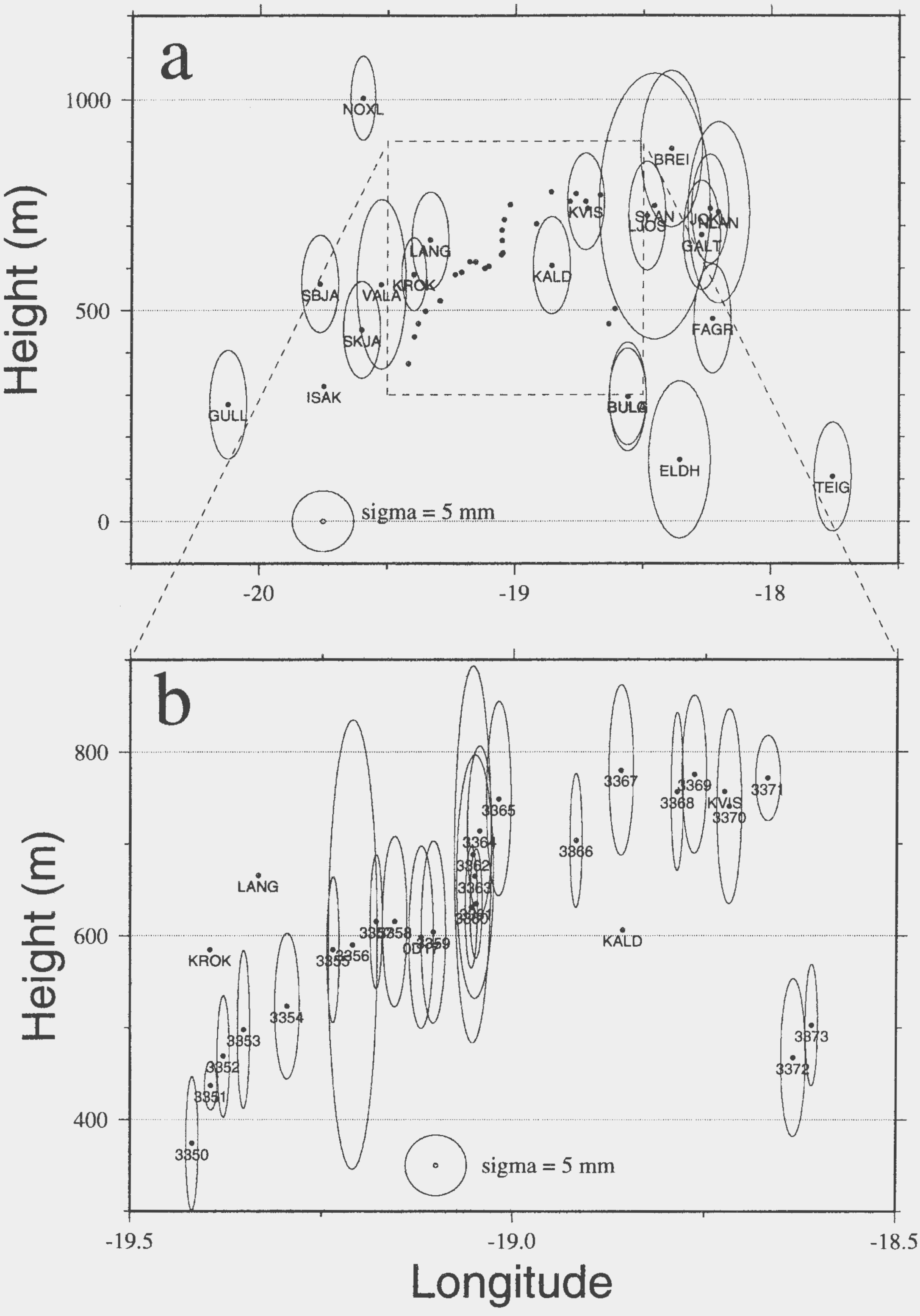

Figure 4.6: Same as Figure 4.2, except for sigmas of the precise orbits and tropospheric parameters coordinate solution.

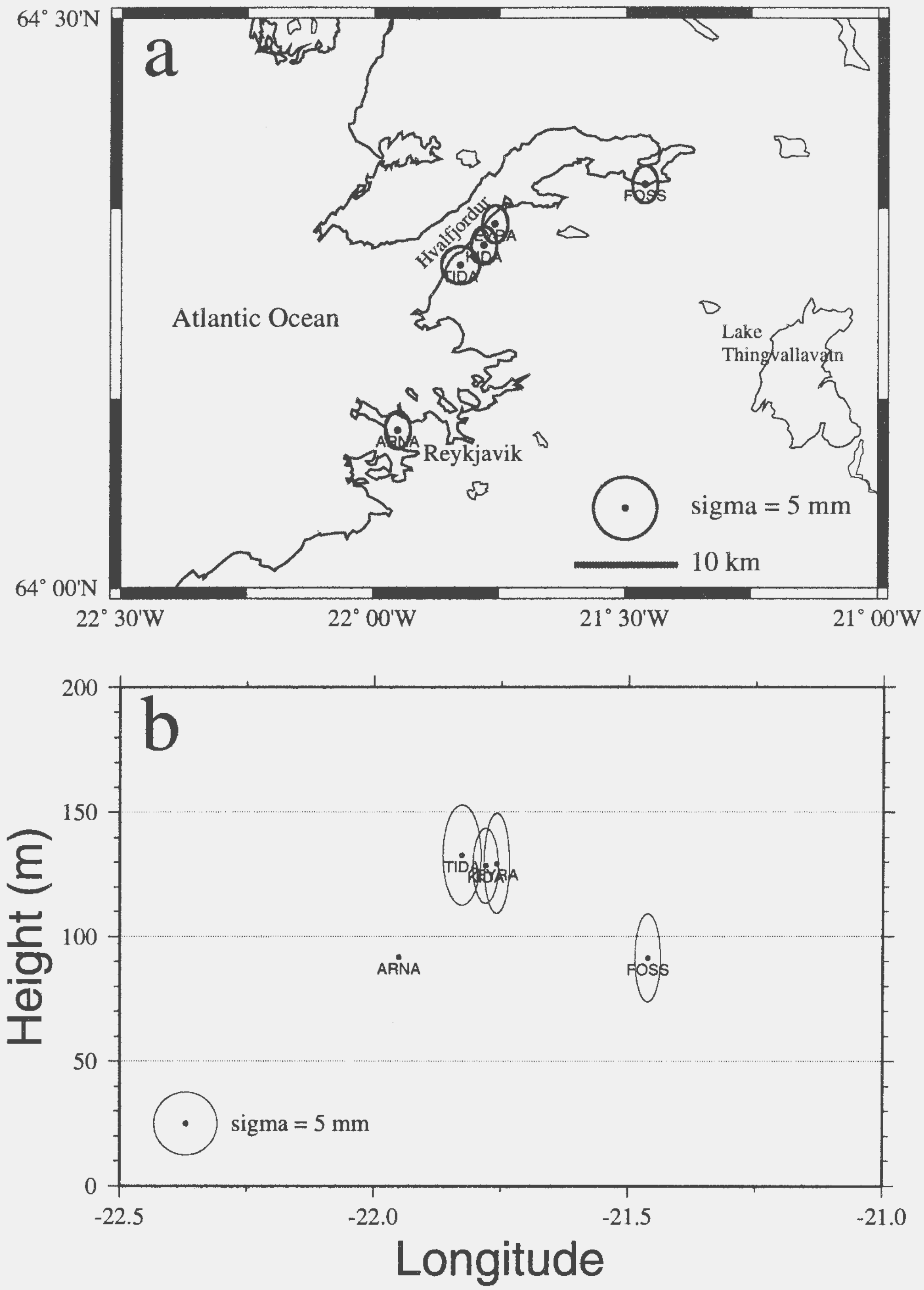

Figure 4.7: Scaled sigmas of the precise orbits coordinate solution for measured stations in Hvalfjörður. Figure a shows horizontal components. On figure b is the height of a station above reference ellipsoid plotted as a function of longitude and ellipses show scaled sigmas in height and east components.

Component	*POS-POTPS (mm)*	*POS-BOS (mm)*	*POTPS-BOS (mm)*
Latitude	0.37	1.92	2.02
Longitude	0.24	2.15	2.22
Height	0.23	4.74	4.96
X	0.46	2.97	3.14
Y	0.27	2.60	2.73
Z	0.37	4.20	4.40
Average	0.32	3.10	3.25

Table 4.4: Average of absolute values of the difference between coordinate solutions. POS = precise orbits solution, POTPS = precise orbits and tropospheric parameters solution, BOS = broadcast orbits solution.

4.4 Comparison of Different Coordinate Results

The difference between produced coordinate sets was calculated. The coordinate solutions obtained from the precise IGS orbits information are in the ITRF-92 reference frame and the broadcast orbits solution is in the WGS-84 coordinate system. Both solutions were calculated by using the ITRF-91 coordinates of the reference station (ISAK). Thus, the final broadcast orbits coordinates are in WGS-84, but translated by the difference between $ISAK_{ITRF-91}$ and $ISAK_{WGS-84}$, which is about $(1.136 \pm 0.132)m$ (Sigmundsson et al. 1995). The final precise orbits coordinates are translated by the difference between $ISAK_{ITRF-91}$ and $ISAK_{ITRF-92}$. The difference between the ITRF-91 and ITRF-92 is less than 2 cm in translation, with no rotation and insignificant scale factor (Boucher et al. 1993).

The average of absolute values of the difference between the coordinate solutions are in Table 4.4. The difference between the two solutions based on precise orbits is an order of magnitude smaller than the difference with the broadcast orbits solution.

A seven-parameter Helmert transformation was calculated between the precise orbits solution and the broadcast orbits solution, see Table 4.5. These parameters indicate the difference between the ITRF-92 and WGS-84 coordinate systems. Corresponding Helmert transformation parameters of the 1992 GPS coordinate solution in South Iceland are also shown (Sigmundsson et al. 1995). The precise orbits solution from 1992 is in the ITRF-91 coordinate system, but the difference between ITRF-91 and ITRF-92 is small, as mentioned above. The difference between the transformation parameters of the two studies, shown in Table 4.5, may be due to better quality of broadcast orbit information in 1994 than in 1992.

Parameter	*This study*	*Sigmundsson et al.*
Number of parameters	7	7
Number of coordinates	138	123
RMS of transformation (m)	0.0045	0.0059
Translation in x (m)	0.343 ± 0.244	-0.824 ± 0.191
Translation in y (m)	-0.323 ± 0.229	-0.777 ± 0.144
Translation in z (m)	-0.316 ± 0.187	-0.090 ± 0.134
Rotation around x axis (arc sec)	0.009 ± 0.007	0.02 ± 0.01
Rotation around y axis (arc sec)	0.015 ± 0.009	-0.02 ± 0.01
Rotation around z axis (arc sec)	0.006 ± 0.005	-0.03 ± 0.01
Scale factor (mm/km)	0.015 ± 0.024	0.05 ± 0.02

Table 4.5: Seven-parameter Helmert transformation between the precise orbits and broadcast orbits coordinate solutions. For comparison are corresponding transformation parameters from Sigmundsson et al. (1995) for the 1992 GPS solutions in South Iceland.

Acknowledgements

The measurements were supported by grants from the Icelandic Science Fund and the Research Fund of the University of Iceland. The National Power Company, Landsvirkjun, provided logistic support.

Heidi Soosalu and Matti Horttanainen participated in the measurements and Þráinn Friðriksson slightly too. Simon D. P. Williams gave useful comments about the graphics.

References

Björnsson, A. (1985), Dynamics of crustal rifting in NE Iceland, *J. Geophys. Res.*, vol. **90**, 10151-10162.

Boucher, C., Z. Altamimi and L. Duhem (1993), ITRF 92 and its associated velocity field, IERS technical note **15**, Paris.

Decker, R. W., P. Einarsson, P. A. Mohr (1971), Rifting in Iceland: New geodetic data. *Science*, vol. **173**, 530-533.

Decker, R. W., P. Einarsson, R. Plumb (1976), Rifting in Iceland: Measuring horizontal movements, Soc. Sci. Islandica, *Greinar*, **V**, 61-67.

Dixon, T. H. (1991), An Introduction to the Global Positioning System and some geological applications, *Reviews of Geophysics*, **29**, 2, 249-276.

Einarsson, P. (1991), Earthquakes and present-day tectonism in Iceland, *Tectonophys.*, **189**, 261-279.

Einarsson, P. (1993), Benchmarks of GPS-measurements in Iceland 1986-1991. The Science Institute of the University of Iceland, report **RH-02-93**, 78 pp.

Erlingsson, S. and P. Einarsson (1995), Distance measurements across the rift zones in southern Iceland, 1967-1986. The Science Institute of the University of Iceland, report **RH-10-95**, 34 pp.

Foulger, G. R., C.-H. Jahn, G. Seeber, P. Einarsson, B. R. Julian and K. Heki (1992), Post rifting stress relaxation at the accretionary plate boundary in Iceland, measured using the Global Positioning System, *Nature*, **358**, 488-490.

Foulger, G. R., G. Beutler, R. Bilham, P. Einarsson, S. Fankhauser, W. Gurtner, U. Hugentobler, W. J. Morgan, M. Rothacher, G. Thorbergsson and U. Wild (1993), The Iceland 1986 GPS geodetic survey: tectonic goals and data processing results. *Bulletin Geodesique*, **67**, 148-172.

Gerke, K., D. Möller, B. Ritter (1978), Geodätische Lagemessungen zur Bestimmung horizontaler Krustenbewegungen in Nordost-Island, in: *Festschrift für Walter Höpcke zum 70. Geburtstag*, 23-33, Hannover.

Gurtner W., G. Mader and D. Arthur (1989), A common exchange format for GPS data, *CSTG GPS Bulletin*, vol. **2**, No. 3, National Geodetic Survey, Rockville.

Hackman, C. (1991), *A study of crustal deformation in Iceland using boundary element modeling and the Global Positioning System.* Ph. D. thesis, University of Colorado, 296 pp.

Hopfield, H. S. (1971), Tropospheric effect on electromagnetically measured range: prediction from surface weather data, *Radio Sci.*, **6**, 357-367.

Kanngieser, E. (1983), Vertical component of ground deformation in north Iceland, *Ann. Geophys.*, **1**, 321-328.

Möller, D., B. Ritter and K. Wendt (1982), Geodetic measurement of horizontal deformations in Northeast Iceland, *Earth Evolution Sciences*, **2**, 149-154.

Rothacher, M., G. Beutler, W. Gurtner, E. Brockmann and L. Mervart (1993), *Documentation for Bernese GPS software version 3.4*, Univ. Bern.

Saastamoinen, J. (1972), Atmospheric correction for the troposphere and stratosphere in radio ranging of satellites. in *The use of artificial satellites for geodesy*, Geophysical Monograph 15, American Geophysical Union, Washington, D.C., 64, 674.

Sigmundsson, F. (1992), *Crustal deformation studies in subaerial parts of the world oceanic rift system: Iceland and Afar*, Ph. D. thesis, University of Colorado, 112 pp.

Sigmundsson, F., P. Einarsson and R. Bilham (1992a), Magma chamber deflation recorded by the Global Positioning System: The Hekla 1991 eruption. *Geophys. Res. Lett.*, vol. **19**, no. 14, 1483-1486.

Sigmundsson, F., P. Einarsson, R. Bilham and S. Sturkell (1992b), South Iceland 1992 GPS-measurements: Summary and daily observation logs. Nordic Volcanological Institute, report **9201**, 19 pp.

Sigmundsson, F. and P. Einarsson (1993a), GPS-monitoring of the Hekla volcano: 1993 field report. Nordic Volcanological Institute.

Sigmundsson, F. and P. Einarsson (1993b), GPS-monitoring of the Mýrdalsjökull volcano: 1993 field report. Nordic Volcanological Institute.

Sigmundsson, F., P. Einarsson, R. Bilham and E. Sturkell (1995), Rift-transform kinematics in south Iceland: Deformation from Global Positioning System measurements, 1986 to 1992. *J. Geophys. Res.*, vol. **100**, no. B4, 6235-6248.

Sigurðsson, O. (1980), Surface deformation of the Krafla fissure swarm in two rifting events, *J. Geophys.*, **47**. 154-159.

Tryggvason, E. (1984), Widening of the Krafla fissure swarm during the 1971-1981 volcano-tectonic episode, *Bull. Volcanol.*, **47**, 47-69.

UNAVCO (1994), *Bernese V3.5 processing with UNAVCO C-shells*, University Navstar Consortium, Boulder, Colorado.

Wendt, K., D. Möller and B. Ritter (1985), Geodetic measurements of surface deformations during the present rifting episode in NE Iceland, *J. Geophys. Res.*, **90**, 10163-10172.

Appendix A

Tables and Plots

A.1 Daily observation logs

Occupation of the GPS Control points are shown on a daily basis in Tables A.1-A.5.

A.2 Plots of Repeatability

Repeatability as a function of baseline length for north, east, height and length components is showed in Figures A.1- A.4.

A.3 Coordinates

Final geocentric and ellipsoidal coordinate solution from the DYNAP program are in Tables A.6-A.13. Scaled sigmas are also shown for the ellipsoidal coordinates.

Date - Day number - Session:															
Site:	05/27 147			05/28 148			05/29 149			05/30 150			05/31 151		
	0	1	2	0	1	2	0	1	2	0	1	2	0	1	2
REYN		x	x	x	x	x	x	x	x	x	x	x	x	x	
ENTA		x	x	x	x										
AUST		x	x	x	x	x									
SOHH						x	x	x							
SOLH						x	x	x	x						
KJAL									x	x	x				
KRIK									x	x	x	x			
OLAF												x	x	x	
RJUP												x	x	x	
	06/02 153			06/03 154			06/04 155			06/05 156			06/06 157		
	0	1	2	0	1	2	0	1	2	0	1	2	0	1	2
SELJ			x	x	x	x	x	x	x	x	x	x	x	x	
HAMR			x	x	x	x	x	x	x	x	x	x	x	x	
STEI				x	x	x	x	x	x	x	x	x	x	x	
	09/18 261			09/19 262			09/20 263			09/21 264			09/22 265		
	0	1	2	0	1	2	0	1	2	0	1	2	0	1	2
REYN		x	x	x	x	x	x	x	x	x	x	x	x	x	
HRIS		x	x	x	x										
HOFD			x	x	x										
SKOG					x	x	x								
FIMM						x	x	x							
STEI									x	x	x				
HAMR									x	x	x				
SELJ												x	x	x	
ALFT												x	x	x	

Table A.1: Occupation of GPS control points near Mýrdalsjökull and Eyjafjallajökull in 1994.

	Date - Day number - Session:																																			
	07/18			07/19			07/20			07/21			07/22			07/23			07/24			07/25			07/26			07/27			07/28			07/29		
	199			200			201			202			203			204			205			206			207			208			209			210		
Site:	0	1	2	0	1	2	0	1	2	0	1	2	0	1	2	0	1	2	0	1	2	0	1	2	0	1	2	0	1	2	0	1	2	0	1	2
ISAK		x	x	x	x	x	x	x	x	x	x	x	x	x	x	x	x	x	x	x	x	x	x	x	x	x	x	x	x	x	x	x	x	x	x	
3359			x	x	x																															
3364			x	x	x																															
3366					x	x	x	x																												
3357						x	x	x																												
3367									x	x	x																									
0D17									x	x	x																									
LJOS												x	x	x																						
JOKU												x	x	x																						
KVIS														x	x	x	x																			
KALD															x	x	x																			
3350																		x	x	x																
LANG																		x	x	x																
THJO																				x	x	x	x													
HAFU																					x	x	x	x												
MOHN																								x	x	x										
LITL																								x	x	x										
SBJA																											x	x	x							
3351																											x	x	x							
SKJA																														x	x	x				
3352																														x	x	x				
3358																																	x	x	x	
3353																																	x	x	x	

Table A.2: Occupation of GPS control points near Hekla and in the Eastern Volcanic Rift Zone in July 1994.

	Date - Day number - Session:																																			
	08/30			08/31			09/01			09/02			09/03			09/04			09/05			09/06			09/07			09/08			09/09			09/10		
	242			243			244			245			246			247			248			249			250			251			252			253		
Site:	0	1	2	0	1	2	0	1	2	0	1	2	0	1	2	0	1	2	0	1	2	0	1	2	0	1	2	0	1	2	0	1	2	0	1	2
ISAK		x	x	x	x	x	x	x	x	x	x	x	x	x	x	x	x	x	x	x	x	x	x	x	x	x	x	x	x	x	x	x	x	x	x	
3361		x	x	x	x																															
3360			x	x	x																															
GALT						x	x	x																												
FAGR						x	x	x																												
ELDH									x	x	x																									
TEIG											x	x	x	x																						
BULA												x	x	x																						
3373														x	x	x	x																			
BULG														x	x	x	x																			
3372																	x	x	x	x																
3371																		x	x	x																
3368																				x	x	x	x													
3369																				x	x	x	x													
3365																								x	x	x										
3363																								x	x	x										
3362																										x	x	x	x							
3356																											x	x	x							
BREI																														x	x	x				
NLAN																														x	x	x				
SLAN																																x	x	x	x	
3370																																	x	x	x	

Table A.3: Occupation of GPS control points in the Eastern Volcanic Rift Zone in August and September 1994.

Date - Day number - Session:																								
	09/10			09/11			09/12			09/13			09/14			09/15			09/16			09/17		
	253			254			255			256			257			258			259			260		
Site:	0	1	2	0	1	2	0	1	2	0	1	2	0	1	2	0	1	2	0	1	2	0	1	2
ISAK			x	x	x	x	x	x	x	x	x	x	x	x	x	x	x	x	x	x	x	x	x	
VALA			x	x	x																			
KROK			x	x	x	x	x	x																
HEKL					x	x																		
NOXL						x	x	x																
3355								x	x	x	x													
3354									x	x	x													
NBJA											x	x	x	x										
PALA												x	x	x	x									
SELS															x	x	x							
DROP															x	x	x							
BRSK																	x	x	x	x				
MUND																		x	x	x				
HEST																					x	x		
RAUD																					x	x	x	

Table A.4: Occupation of GPS control points near Hekla Volcano and in the Eastern Volcanic Rift Zone in September 1994.

Date - Day number - Session:															
	10/31			11/01			11/03			11/04			11/05		
	304			305			307			308			309		
	0	1	2	0	1	2	0	1	2	0	1	2	0	1	2
ISAK		x	x	x	x										
GULL			x	x	x										
ARNA								x	x	x	x	x	x	x	
TIDA								x	x	x	x				
KIDA								x	x	x	x				
EYRA											x	x	x		
FOSS											x	x	x	x	

Table A.5: Occupation of GPS control points in October and November 1994.

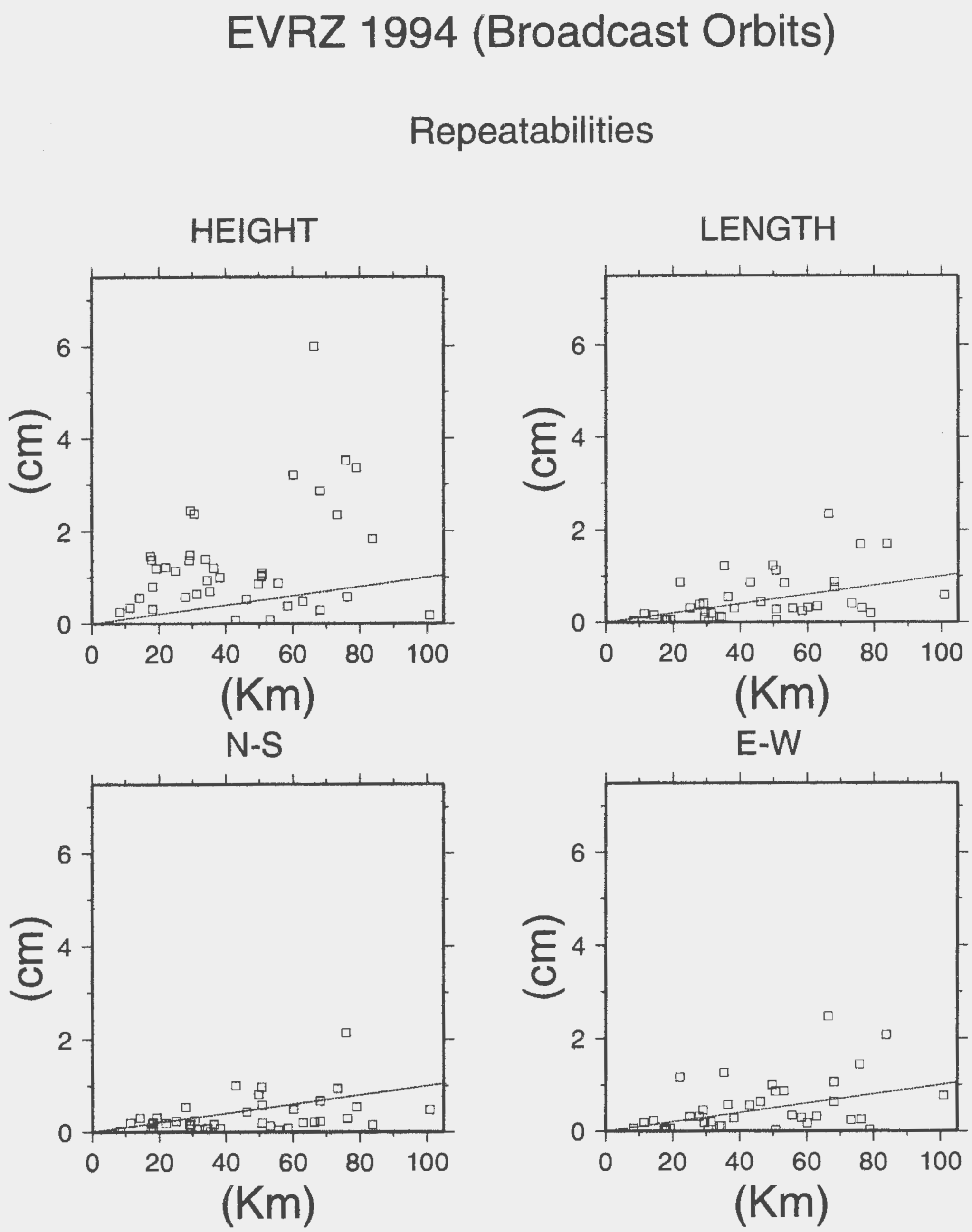

Figure A.1: Plots of repeatability as a function of baseline length of the north, east, height and length components for the broadcast orbits coordinate solutions of the measurements in the Eastern Volcanic Rift Zone (EVRZ). The lines correspond to 0.1 ppm.

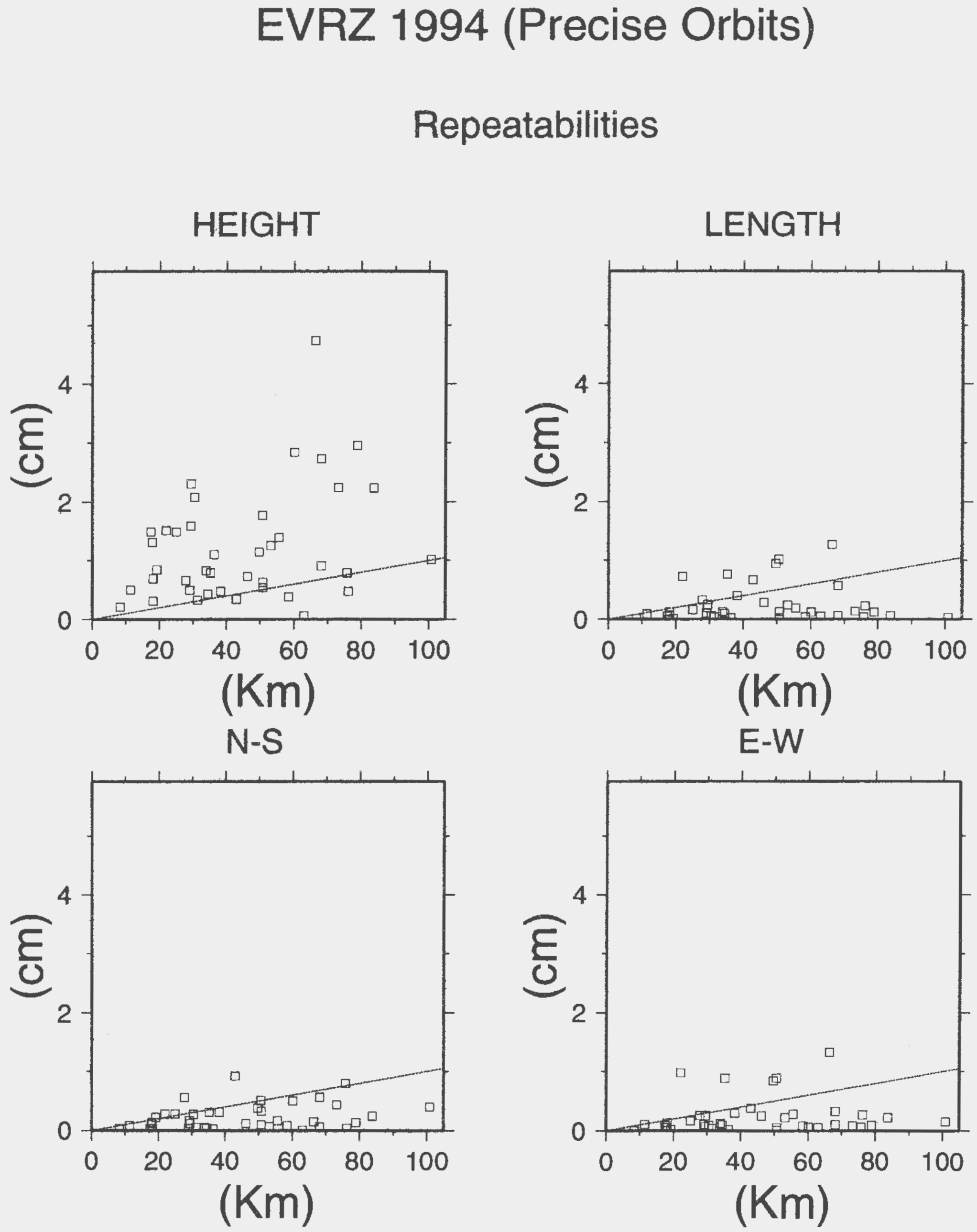

Figure A.2: Plots of repeatability as a function of baseline length of the north, east, height and length components for the precise orbits coordinate solutions.

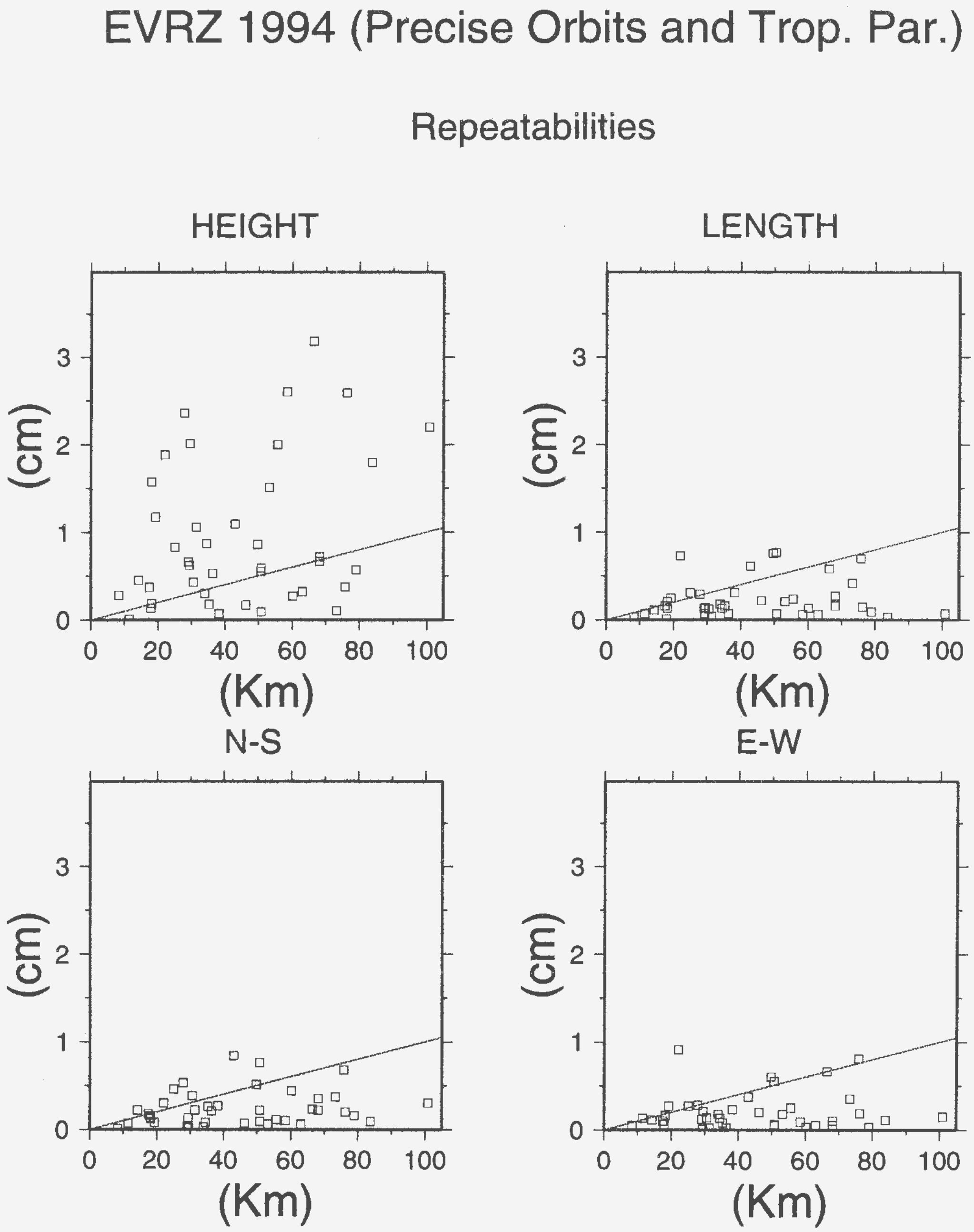

Figure A.3: Plots of repeatability as a function of baseline length of the north, east, height and length components for the precise orbits and tropospheric parameters coordinate solutions.

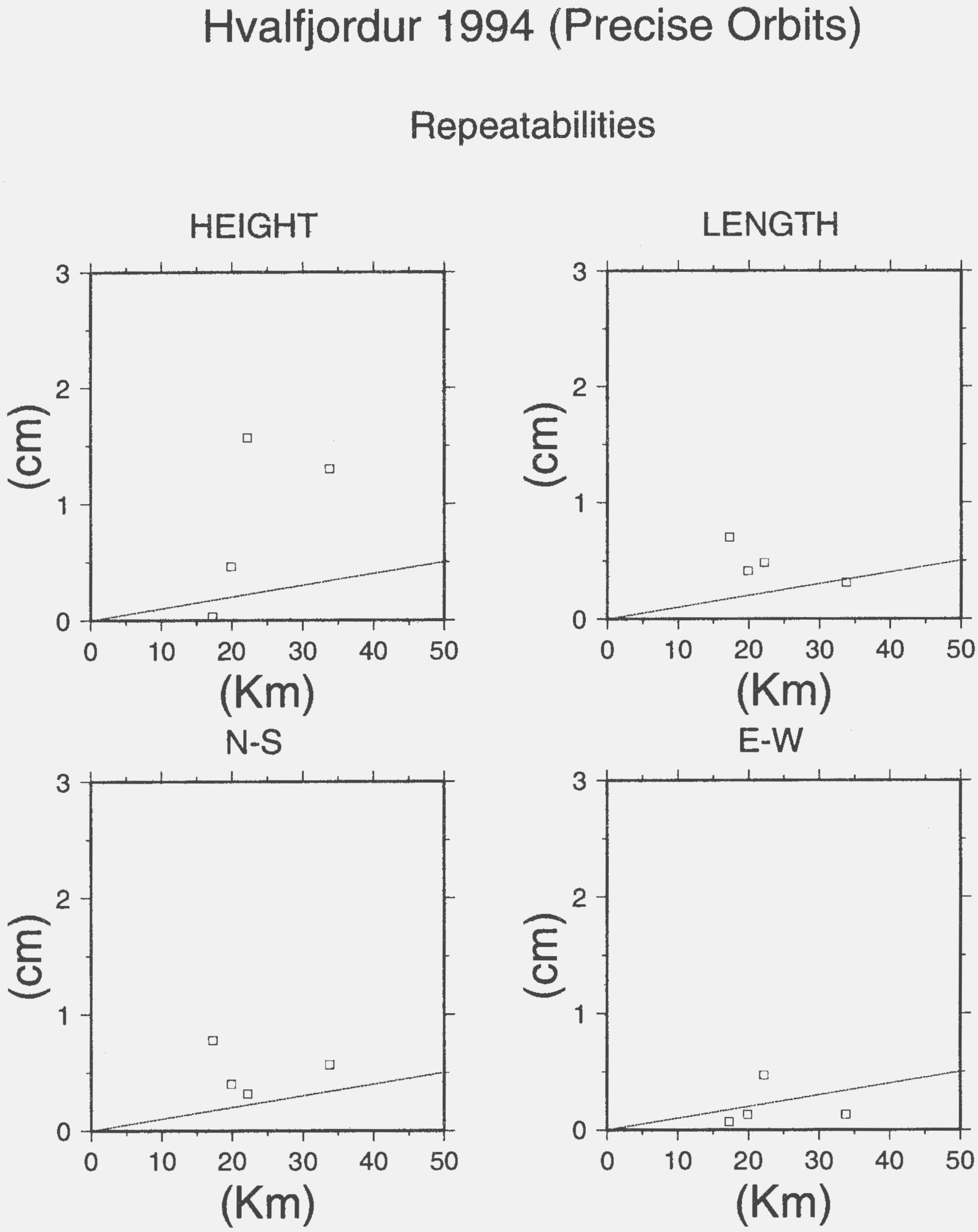

Figure A.4: Plots of repeatability as a function of baseline length of the north, east, height and length components for the precise orbits coordinate solutions of the Hvalfjörður measurements.

num	*Station*	*X (m)*	*Y (m)*	*Z (m)*	*flag*
2	3359	2640063.1913	-914420.6733	5715079.4985	p
3	3364	2649476.9414	-914584.3101	5710846.8588	p
4	ISAK	2627583.7747	-943252.6851	5715821.0364	f
5	3357	2638998.8022	-917914.4904	5715024.0694	p
6	3366	2653319.9080	-909384.4290	5709887.9272	p
7	0D17	2637226.8701	-914253.6612	5716400.3127	p
8	3367	2655652.9143	-907160.9432	5709246.9492	p
9	JOKU	2633520.9091	-867895.7525	5725425.9096	p
10	LJOS	2635613.7710	-881121.4084	5722443.5420	p
11	KALD	2619303.0698	-894604.9123	5727671.6328	p
12	KVIS	2635844.4163	-893464.4249	5720473.7671	p
13	3350	2626895.4505	-926059.2720	5718987.7213	p
14	LANG	2616363.0962	-917915.0463	5725407.9625	p
15	3351	2629170.3160	-925601.8097	5718092.8621	p
16	SBJA	2637091.6944	-947497.4864	5711042.0147	p
17	3352	2631269.3149	-925495.9913	5717186.2155	p
18	SKJA	2633732.1199	-937792.1206	5714051.9643	p
19	3353	2633096.8348	-924768.6048	5716499.7736	p
20	3358	2639839.7890	-916960.8801	5714790.4478	p
21	3360	2641413.7637	-912336.0311	5714820.5258	p
22	3361	2643121.0596	-912620.3552	5713995.8523	p
23	FAGR	2674296.6320	-880798.7727	5704367.2746	p
24	GALT	2662698.4592	-879191.3126	5710219.7540	p
25	ELDH	2690916.2659	-892918.7029	5694351.0775	p
26	BULA	2676652.7577	-898688.3020	5700290.7961	p
27	TEIG	2681361.8032	-858751.7285	5703994.5199	p
28	3373	2665430.8182	-897576.7163	5705916.1422	p
29	BULG	2676670.8833	-898727.0722	5700276.3561	p
30	3371	2660248.0686	-898807.3294	5708424.7567	p
31	3372	2663579.2216	-898189.8210	5706639.6073	p
32	3368	2657038.0807	-903852.3509	5709102.0368	p
33	3369	2657239.4366	-902762.9530	5709201.1730	p
34	3363	2647077.1744	-914049.9088	5711981.8352	p
35	3365	2651581.8386	-914016.9626	5710005.6965	p
36	3356	2638863.8972	-919448.3489	5714812.9887	p
37	3362	2644938.5630	-913455.3215	5713086.9038	p
38	3354	2635112.8018	-922547.4540	5715961.7041	p
39	3355	2637288.8809	-920218.9781	5715405.9110	p
40	BREI	2643349.1330	-878870.9629	5719418.9474	p
41	NLAN	2642174.4338	-869033.7088	5721283.2771	p
42	3370	2659104.4759	-901038.8737	5708570.3496	p
43	SLAN	2649577.6856	-884297.7640	5715573.3379	p
44	KROK	2638462.4742	-928944.8620	5713465.7003	p
45	VALA	2635388.9597	-934419.6658	5713961.4451	p
46	NOXL	2640714.5638	-940158.5686	5711074.4218	p
47	GULL	2601725.4781	-953207.1237	5725874.2320	p

Table A.6: The geocentric coordinates from DYNAP of the broadcast orbits solution. The coordinates are in WGS-84 coordinate system, but translated, see Section 4.4.

num	*Station*	*Latitude*	*Longitude*	*Height (m)*	σ_{lat} *(m)*	σ_{lon} *(m)*	σ_h *(m)*
1	3359	64.09882992	-19.10420171	604.0890	0.0040	0.0030	0.0100
2	3364	64.01003142	-19.04438167	713.9970	0.0040	0.0030	0.0100
3	ISAK	64.11932526	-19.74717433	319.2890	0.0000	0.0000	0.0000
4	3357	64.09748238	-19.17904412	615.4270	0.0040	0.0030	0.0080
5	3366	63.99059964	-18.91835943	703.7210	0.0030	0.0030	0.0080
6	0D17	64.12606946	-19.12001750	598.3910	0.0040	0.0030	0.0100
7	3367	63.97608754	-18.85997207	780.1780	0.0040	0.0030	0.0090
8	JOKU	64.30955334	-18.24000741	740.2970	0.0040	0.0030	0.0090
9	LJOS	64.24822743	-18.48548024	723.6970	0.0040	0.0030	0.0090
10	KALD	64.35855992	-18.85724798	606.2271	0.0040	0.0030	0.0080
11	KVIS	64.20697331	-18.72496592	757.1320	0.0030	0.0030	0.0080
12	3350	64.18346372	-19.41907951	373.8420	0.0030	0.0020	0.0080
13	LANG	64.31057890	-19.33272037	665.3760	0.0030	0.0030	0.0080
14	3351	64.16387108	-19.39466397	436.8689	0.0030	0.0020	0.0070
15	SBJA	64.01682333	-19.76317896	562.0010	0.0030	0.0030	0.0080
16	3352	64.14462614	-19.37829588	468.7760	0.0030	0.0020	0.0080
17	SKJA	64.08051306	-19.59927210	453.7730	0.0030	0.0030	0.0080
18	3353	64.12997122	-19.35175909	497.9680	0.0030	0.0030	0.0080
19	3358	64.09268388	-19.15491330	615.5390	0.0030	0.0030	0.0080
20	3360	64.09301491	-19.05475192	631.0510	0.0030	0.0020	0.0070
21	3361	64.07601432	-19.04883764	635.1620	0.0030	0.0020	0.0060
22	FAGR	63.88199124	-18.22966924	480.4260	0.0040	0.0030	0.0090
23	GALT	63.99786357	-18.27260771	677.8390	0.0040	0.0030	0.0090
24	ELDH	63.68469753	-18.35723846	146.1370	0.0060	0.0050	0.0130
25	BULA	63.80241820	-18.55951781	295.7380	0.0040	0.0030	0.0090
26	TEIG	63.88125344	-17.75854806	105.6060	0.0040	0.0030	0.0090
27	3373	63.91315519	-18.61081508	502.9850	0.0040	0.0030	0.0090
28	BULG	63.80212339	-18.56014656	295.8150	0.0040	0.0030	0.0080
29	3371	63.95944184	-18.66836168	771.5980	0.0050	0.0040	0.0110
30	3372	63.92856716	-18.63470328	467.4970	0.0050	0.0040	0.0110
31	3368	63.97355420	-18.78691271	756.8240	0.0040	0.0030	0.0090
32	3369	63.97523391	-18.76453250	775.7050	0.0040	0.0030	0.0090
33	3363	64.03418716	-19.05006724	664.3020	0.0070	0.0050	0.0150
34	3365	63.99217413	-19.01939507	749.1120	0.0050	0.0040	0.0120
35	3356	64.09361444	-19.20965654	590.2060	0.0090	0.0070	0.0220
36	3362	64.05639312	-19.05285207	688.2530	0.0070	0.0060	0.0170
37	3354	64.11844351	-19.29504310	523.3320	0.0040	0.0030	0.0080
38	3355	64.10588991	-19.23521384	584.7790	0.0030	0.0020	0.0070
39	BREI	64.18291137	-18.39113433	882.6730	0.0060	0.0050	0.0130
40	NLAN	64.22413581	-18.20647644	731.7650	0.0070	0.0050	0.0150
41	3370	63.96298109	-18.71897557	740.8530	0.0060	0.0050	0.0130
42	SLAN	64.10633074	-18.45645562	747.0320	0.0090	0.0090	0.0220
43	KROK	64.06606393	-19.39605003	585.0390	0.0030	0.0020	0.0060
44	VALA	64.07667243	-19.52278263	561.2400	0.0060	0.0040	0.0140
45	NOXL	64.00937408	-19.59696545	1002.8930	0.0030	0.0020	0.0070
46	GULL	64.32747535	-20.12157031	276.9130	0.0040	0.0030	0.0090

Table A.7: The ellipsoidal coordinates and scaled sigmas of the broadcast orbits solution. The coordinates are in the WGS-84 coordinate system, but translated, see Section 4.4.

num	*Station*	*X (m)*	*Y (m)*	*Z (m)*	*flag*
2	3359	2640063.1970	-914420.6753	5715079.5067	p
3	3364	2649476.9497	-914584.3098	5710846.8661	p
4	ISAK	2627583.7747	-943252.6851	5715821.0364	f
5	3357	2638998.8073	-917914.4915	5715024.0779	p
6	3366	2653319.9127	-909384.4312	5709887.9357	p
7	0D17	2637226.8695	-914253.6603	5716400.3131	p
8	3367	2655652.9155	-907160.9465	5709246.9481	p
9	JOKU	2633520.9068	-867895.7492	5725425.9000	p
10	LJOS	2635613.7675	-881121.4054	5722443.5329	p
11	KALD	2619303.0752	-894604.9114	5727671.6415	p
12	KVIS	2635844.4174	-893464.4241	5720473.7667	p
13	3350	2626895.4516	-926059.2714	5718987.7209	p
14	LANG	2616363.0977	-917915.0444	5725407.9621	p
15	3351	2629170.3166	-925601.8099	5718092.8619	p
16	SBJA	2637091.6943	-947497.4867	5711042.0147	p
17	3352	2631269.3151	-925495.9901	5717186.2157	p
18	SKJA	2633732.1197	-937792.1202	5714051.9645	p
19	3353	2633096.8344	-924768.6050	5716499.7737	p
20	3358	2639839.7894	-916960.8817	5714790.4474	p
21	3360	2641413.7666	-912336.0324	5714820.5253	p
22	3361	2643121.0666	-912620.3582	5713995.8609	p
23	FAGR	2674296.6327	-880798.7762	5704367.2748	p
24	GALT	2662698.4662	-879191.3152	5710219.7615	p
25	ELDH	2690916.2747	-892918.7006	5694351.0804	p
26	BULA	2676652.7612	-898688.2968	5700290.7897	p
27	TEIG	2681361.7952	-858751.7176	5703994.5130	p
28	3373	2665430.8212	-897576.7190	5705916.1560	p
29	BULG	2676670.8857	-898727.0766	5700276.3699	p
30	3371	2660248.0668	-898807.3274	5708424.7568	p
31	3372	2663579.2191	-898189.8186	5706639.6066	p
32	3368	2657038.0855	-903852.3519	5709102.0467	p
33	3369	2657239.4368	-902762.9522	5709201.1742	p
34	3363	2647077.1727	-914049.9126	5711981.8365	p
35	3365	2651581.8437	-914016.9670	5710005.7058	p
36	3356	2638863.8958	-919448.3478	5714812.9895	p
37	3362	2644938.5596	-913455.3184	5713086.9070	p
38	3354	2635112.8017	-922547.4538	5715961.7031	p
39	3355	2637288.8800	-920218.9785	5715405.9102	p
40	BREI	2643349.1335	-878870.9642	5719418.9514	p
41	NLAN	2642174.4334	-869033.7032	5721283.2848	p
42	3370	2659104.4657	-901038.8618	5708570.3439	p
43	SLAN	2649577.6795	-884297.7775	5715573.3398	p
44	KROK	2638462.4700	-928944.8608	5713465.6935	p
45	VALA	2635388.9632	-934419.6672	5713961.4544	p
46	NOXL	2640714.5642	-940158.5706	5711074.4212	p
47	GULL	2601725.4790	-953207.1229	5725874.2317	p

Table A.8: The geocentric coordinates from DYNAP of the precise orbits solution. The coordinates are in the ITRF-92 reference frame.

num	Station	Latitude	Longitude	Height (m)	σ_{lat} (m)	σ_{lon} (m)	σ_h (m)
1	3359	64.09882990	-19.10420171	604.0990	0.0030	0.0030	0.0080
2	3364	64.01003139	-19.04438161	714.0070	0.0030	0.0030	0.0080
3	ISAK	64.11932526	-19.74717433	319.2890	0.0000	0.0000	0.0000
4	3357	64.09748237	-19.17904411	615.4370	0.0030	0.0020	0.0060
5	3366	63.99059963	-18.91835944	703.7309	0.0030	0.0020	0.0060
6	0D17	64.12606947	-19.12001749	598.3910	0.0030	0.0030	0.0070
7	3367	63.97608752	-18.85997212	780.1780	0.0030	0.0020	0.0070
8	JOKU	64.30955333	-18.24000736	740.2870	0.0030	0.0020	0.0060
9	LJOS	64.24822743	-18.48548020	723.6870	0.0030	0.0020	0.0070
10	KALD	64.35855991	-18.85724792	606.2370	0.0030	0.0020	0.0060
11	KVIS	64.20697330	-18.72496589	757.1320	0.0020	0.0020	0.0050
12	3350	64.18346371	-19.41907949	373.8420	0.0020	0.0020	0.0060
13	LANG	64.31057889	-19.33272032	665.3760	0.0020	0.0020	0.0060
14	3351	64.16387107	-19.39466397	436.8690	0.0020	0.0020	0.0050
15	SBJA	64.01682333	-19.76317896	562.0010	0.0030	0.0020	0.0060
16	3352	64.14462614	-19.37829586	468.7760	0.0030	0.0020	0.0060
17	SKJA	64.08051306	-19.59927209	453.7730	0.0030	0.0020	0.0060
18	3353	64.12997122	-19.35175910	497.9680	0.0030	0.0020	0.0060
19	3358	64.09268387	-19.15491333	615.5390	0.0030	0.0020	0.0060
20	3360	64.09301488	-19.05475192	631.0520	0.0020	0.0020	0.0050
21	3361	64.07601429	-19.04883765	635.1730	0.0020	0.0020	0.0050
22	FAGR	63.88199123	-18.22966930	480.4270	0.0030	0.0020	0.0070
23	GALT	63.99786354	-18.27260772	677.8490	0.0030	0.0020	0.0070
24	ELDH	63.68469748	-18.35723836	146.1430	0.0040	0.0030	0.0100
25	BULA	63.80241816	-18.55951768	295.7330	0.0030	0.0020	0.0070
26	TEIG	63.88125350	-17.75854790	105.5950	0.0030	0.0020	0.0060
27	3373	63.91315522	-18.61081512	502.9990	0.0030	0.0020	0.0070
28	BULG	63.80212341	-18.56014663	295.8290	0.0030	0.0020	0.0060
29	3371	63.95944186	-18.66836165	771.5970	0.0040	0.0030	0.0090
30	3372	63.92856718	-18.63470325	467.4950	0.0040	0.0030	0.0090
31	3368	63.97355420	-18.78691269	756.8351	0.0030	0.0020	0.0070
32	3369	63.97523392	-18.76453249	775.7060	0.0030	0.0030	0.0080
33	3363	64.03418717	-19.05006732	664.3030	0.0050	0.0040	0.0110
34	3365	63.99217412	-19.01939512	749.1231	0.0040	0.0030	0.0090
35	3356	64.09361446	-19.20965653	590.2060	0.0070	0.0050	0.0170
36	3362	64.05639316	-19.05285203	688.2541	0.0050	0.0040	0.0130
37	3354	64.11844351	-19.29504309	523.3310	0.0030	0.0020	0.0070
38	3355	64.10588991	-19.23521385	584.7780	0.0020	0.0020	0.0060
39	BREI	64.18291137	-18.39113435	882.6770	0.0040	0.0040	0.0110
40	NLAN	64.22413586	-18.20647634	731.7710	0.0050	0.0040	0.0120
41	3370	63.96298118	-18.71897541	740.8420	0.0040	0.0030	0.0100
42	SLAN	64.10633076	-18.45645593	747.0330	0.0070	0.0060	0.0180
43	KROK	64.06606394	-19.39605004	585.0310	0.0020	0.0020	0.0050
44	VALA	64.07667244	-19.52278263	561.2500	0.0040	0.0030	0.0110
45	NOXL	64.00937407	-19.59696549	1002.8930	0.0030	0.0020	0.0060
46	GULL	64.32747535	-20.12157029	276.9130	0.0030	0.0020	0.0070

Table A.9: The ellipsoidal coordinates and scaled sigmas of the precise orbits solution. The coordinates are in the ITRF-92 reference frame.

num	*Station*	*X (m)*	*Y (m)*	*Z (m)*	*flag*
2	3359	2640063.1972	-914420.6755	5715079.5065	p
3	3364	2649476.9496	-914584.3101	5710846.8661	p
4	ISAK	2627583.7747	-943252.6851	5715821.0364	f
5	3357	2638998.8070	-917914.4915	5715024.0781	p
6	3366	2653319.9145	-909384.4312	5709887.9349	p
7	0D17	2637226.8656	-914253.6590	5716400.3040	p
8	3367	2655652.9157	-907160.9460	5709246.9481	p
9	JOKU	2633520.9068	-867895.7491	5725425.9000	p
10	LJOS	2635613.7675	-881121.4054	5722443.5329	p
11	KALD	2619303.0743	-894604.9115	5727671.6419	p
12	KVIS	2635844.4178	-893464.4238	5720473.7666	p
13	3350	2626895.4524	-926059.2717	5718987.7205	p
14	LANG	2616363.0980	-917915.0445	5725407.9619	p
15	3351	2629170.3158	-925601.8096	5718092.8623	p
16	SBJA	2637091.6943	-947497.4868	5711042.0147	p
17	3352	2631269.3154	-925495.9899	5717186.2155	p
18	SKJA	2633732.1200	-937792.1202	5714051.9643	p
19	3353	2633096.8334	-924768.6052	5716499.7741	p
20	3358	2639839.7892	-916960.8820	5714790.4474	p
21	3360	2641413.7677	-912336.0327	5714820.5248	p
22	3361	2643121.0671	-912620.3584	5713995.8606	p
23	FAGR	2674296.6331	-880798.7761	5704367.2747	p
24	GALT	2662698.4662	-879191.3152	5710219.7615	p
25	ELDH	2690916.2739	-892918.7003	5694351.0808	p
26	BULA	2676652.7617	-898688.2963	5700290.7896	p
27	TEIG	2681361.7955	-858751.7167	5703994.5130	p
28	3373	2665430.8203	-897576.7188	5705916.1564	p
29	BULG	2676670.8856	-898727.0761	5700276.3700	p
30	3371	2660248.0672	-898807.3269	5708424.7567	p
31	3372	2663579.2192	-898189.8184	5706639.6066	p
32	3368	2657038.0848	-903852.3531	5709102.0468	p
33	3369	2657239.4360	-902762.9519	5709201.1746	p
34	3363	2647077.1726	-914049.9121	5711981.8366	p
35	3365	2651581.8435	-914016.9676	5710005.7058	p
36	3356	2638863.8958	-919448.3478	5714812.9895	p
37	3362	2644938.5596	-913455.3184	5713086.9070	p
38	3354	2635112.8020	-922547.4538	5715961.7029	p
39	3355	2637288.8800	-920218.9785	5715405.9102	p
40	BREI	2643349.1334	-878870.9644	5719418.9514	p
41	NLAN	2642174.4340	-869033.7034	5721283.2845	p
42	3370	2659104.4648	-901038.8618	5708570.3443	p
43	SLAN	2649577.6795	-884297.7775	5715573.3398	p
44	KROK	2638462.4698	-928944.8607	5713465.6936	p
45	VALA	2635388.9635	-934419.6672	5713961.4543	p
46	NOXL	2640714.5642	-940158.5706	5711074.4212	p
47	GULL	2601725.4790	-953207.1220	5725874.2319	p

Table A.10: The geocentric coordinates from DYNAP of the precise orbits and tropospheric parameters solution. The coordinates are in the ITRF-92 reference frame.

num	*Station*	*Latitude*	*Longitude*	*Height (m)*	σ_{lat} *(m)*	σ_{lon} *(m)*	σ_h *(m)*
1	3359	64.09882990	-19.10420171	604.0990	0.0020	0.0020	0.0150
2	3364	64.01003139	-19.04438162	714.0070	0.0020	0.0020	0.0140
3	ISAK	64.11932526	-19.74717433	319.2890	0.0000	0.0000	0.0000
4	3357	64.09748237	-19.17904411	615.4370	0.0020	0.0010	0.0110
5	3366	63.99059962	-18.91835943	703.7310	0.0020	0.0010	0.0110
6	0D17	64.12606946	-19.12001749	598.3810	0.0020	0.0020	0.0150
7	3367	63.97608752	-18.85997211	780.1780	0.0020	0.0020	0.0140
8	JOKU	64.30955333	-18.24000735	740.2870	0.0020	0.0010	0.0120
9	LJOS	64.24822743	-18.48548020	723.6870	0.0020	0.0010	0.0130
10	KALD	64.35855992	-18.85724793	606.2370	0.0020	0.0010	0.0110
11	KVIS	64.20697330	-18.72496589	757.1320	0.0010	0.0010	0.0090
12	3350	64.18346371	-19.41907949	373.8420	0.0020	0.0010	0.0110
13	LANG	64.31057889	-19.33272032	665.3760	0.0020	0.0010	0.0110
14	3351	64.16387108	-19.39466397	436.8690	0.0020	0.0010	0.0040
15	SBJA	64.01682333	-19.76317897	562.0010	0.0020	0.0010	0.0050
16	3352	64.14462614	-19.37829585	468.7760	0.0020	0.0010	0.0100
17	SKJA	64.08051306	-19.59927209	453.7730	0.0020	0.0010	0.0110
18	3353	64.12997123	-19.35175911	497.9680	0.0020	0.0010	0.0130
19	3358	64.09268388	-19.15491333	615.5389	0.0020	0.0020	0.0140
20	3360	64.09301487	-19.05475192	631.0520	0.0020	0.0010	0.0100
21	3361	64.07601428	-19.04883765	635.1730	0.0010	0.0010	0.0090
22	FAGR	63.88199123	-18.22966929	480.4271	0.0020	0.0010	0.0120
23	GALT	63.99786354	-18.27260772	677.8490	0.0020	0.0020	0.0130
24	ELDH	63.68469749	-18.35723836	146.1430	0.0030	0.0030	0.0240
25	BULA	63.80241816	-18.55951767	295.7330	0.0020	0.0010	0.0110
26	TEIG	63.88125350	-17.75854788	105.5950	0.0020	0.0010	0.0110
27	3373	63.91315523	-18.61081512	502.9990	0.0020	0.0010	0.0100
28	BULG	63.80212341	-18.56014662	295.8290	0.0010	0.0010	0.0100
29	3371	63.95944186	-18.66836164	771.5970	0.0020	0.0020	0.0070
30	3372	63.92856718	-18.63470324	467.4950	0.0020	0.0020	0.0130
31	3368	63.97355420	-18.78691272	756.8350	0.0020	0.0010	0.0130
32	3369	63.97523393	-18.76453249	775.7060	0.0020	0.0020	0.0130
33	3363	64.03418717	-19.05006732	664.3030	0.0030	0.0030	0.0200
34	3365	63.99217412	-19.01939513	749.1231	0.0030	0.0020	0.0160
35	3356	64.09361446	-19.20965653	590.2060	0.0050	0.0040	0.0370
36	3362	64.05639316	-19.05285203	688.2541	0.0040	0.0030	0.0310
37	3354	64.11844350	-19.29504309	523.3310	0.0020	0.0020	0.0120
38	3355	64.10588991	-19.23521385	584.7780	0.0020	0.0010	0.0120
39	BREI	64.18291138	-18.39113436	882.6770	0.0030	0.0020	0.0200
40	NLAN	64.22413585	-18.20647634	731.7710	0.0030	0.0030	0.0210
41	3370	63.96298119	-18.71897541	740.8420	0.0020	0.0020	0.0160
42	SLAN	64.10633076	-18.45645593	747.0330	0.0040	0.0030	0.0260
43	KROK	64.06606394	-19.39605004	585.0310	0.0010	0.0010	0.0050
44	VALA	64.07667244	-19.52278263	561.2500	0.0030	0.0020	0.0210
45	NOXL	64.00937407	-19.59696549	1002.8930	0.0010	0.0010	0.0090
46	GULL	64.32747535	-20.12157027	276.9130	0.0020	0.0020	0.0140

Table A.11: The ellipsoidal coordinates and scaled sigmas of the precise orbits and troposheric parameters solution. The coordinates are in the ITRF-92 reference frame.

num	*Station*	*X (m)*	*Y (m)*	*Z (m)*	*flag*
2	ARNA	2587441.6610	-1042831.2440	5716573.5553	f
3	KIDA	2575455.7723	-1029103.7779	5724456.1973	p
4	TIDA	2576210.4830	-1031841.6063	5723634.0073	p
5	EYRA	2574120.3528	-1027424.3139	5725353.4663	p
6	FOSS	2576133.6445	-1012786.1396	5727002.2659	p

Table A.12: The geocentric coordinates form DYNAP of the precise orbits solution of the Hvalfjörður Measurements. The coordinates are in the ITRF-92 reference frame.

num	*Station*	*Latitude*	*Longitude*	*Height (m)*	σ_{lat} *(m)*	σ_{lon} *(m)*	σ_h *(m)*
1	ARNA	64.13900245	-21.95119219	91.8160	0.0000	0.0000	0.0000
2	KIDA	64.30089799	-21.78072211	128.4820	0.0030	0.0020	0.0060
3	TIDA	64.28381681	-21.82743003	132.7500	0.0030	0.0030	0.0080
4	EYRA	64.31944642	-21.75872539	129.4270	0.0030	0.0020	0.0080
5	FOSS	64.35430553	-21.46187018	91.4250	0.0030	0.0020	0.0070

Table A.13: The ellipsoidal coordinates and scaled sigmas of a precise orbits solution of the Hvalfjörður data. The coordinates are in the ITRF-92 reference frame.